nature microbiology

ARTICLES

https://doi.org/10.1038/s41564-019-0658-4

Klebsiella michiganensis transmission enhances resistance to Enterobacteriaceae gut invasion by nutrition competition

Rita A. Oliveira[1], Katharine M. Ng[2], Margarida B. Correia[1], Vitor Cabral[1], Handuo Shi[2], Justin L. Sonnenburg[3,4], Kerwyn Casey Huang[2,3,4] and Karina B. Xavier[1*]

Intestinal microbiotas contain beneficial microorganisms that protect against pathogen colonization; treatment with antibiotics disrupts the microbiota and compromises colonization resistance. Here, we determine the impact of exchanging microorganisms between hosts on resilience to the colonization of invaders after antibiotic-induced dysbiosis. We assess the functional consequences of dysbiosis using a mouse model of colonization resistance against *Escherichia coli*. Antibiotics caused stochastic loss of members of the microbiota, but the microbiotas of co-housed mice remained more similar to each other compared with the microbiotas among singly housed animals. Strikingly, co-housed mice maintained colonization resistance after treatment with antibiotics, whereas most singly housed mice were susceptible to *E. coli*. The ability to retain or share the commensal *Klebsiella michiganensis*, a member of the Enterobacteriaceae family, was sufficient for colonization resistance after treatment with antibiotics. *K. michiganensis* generally outcompeted *E. coli* in vitro, but in vivo administration of galactitol—a nutrient that supports the growth of only *E. coli*—to bi-colonized gnotobiotic mice abolished the colonization-resistance capacity of *K. michiganensis* against *E. coli*, supporting the idea that nutrient competition is the primary interaction mechanism. *K. michiganensis* also hampered colonization of the pathogen *Salmonella*, prolonging host survival. Our results address functional consequences of the stochastic effects of microbiota perturbations, whereby microbial transmission through host interactions can facilitate reacquisition of beneficial commensals, minimizing the negative impact of antibiotics.

To remain healthy, mammals rely on their microbiome. The intestinal microbiome is essential for host nutrition and immunity[1–3], and for resisting pathogen colonization and pathobiont expansion[4–6]. In humans, diverse gut microbiotas are usually highly stable[7], but drug treatments such as antibiotics negatively affect gut commensals and pathogens alike[8–11], thereby increasing host susceptibility to a wide range of bacterial infections[12–15]. Mechanisms of colonization-resistance against particular taxonomic groups such as Proteobacteria and Firmicutes[4,16] mainly involve competition for nutritional niches[17–20], production of inhibitory and signalling molecules[21–29], and contact-dependent killing[30,31]. Transmission through interhost interactions promotes the maintenance of commensal microorganisms and has important roles in microbiota resilience against invaders[32], as previously shown in both cohabiting mice[33] and humans[34]. During treatment with antibiotics, transmission can play a critical role in the recolonization of important species that are stochastically eliminated; such events rely on the presence of key microorganisms within the environmental reservoir and, therefore, depend on the degree of interactions among hosts[35–37].

Here we studied the effect of cohabitation on microbiota resilience to invasion. We observed that the aggregate microbiota reservoir in co-housed animals resulted in increased colonization resistance after antibiotic-induced dysbiosis compared with the colonization resistance in singly housed animals. Antibiotics treatment of singly housed mice resulted in stochastic losses among members of Proteobacteria, whereas co-housed mice were able to maintain the members of this phylum, indicating that this stochastic extinction was attenuated by the environmental reservoir. The Proteobacterium *K. michiganensis* was sufficient for colonization resistance against an invading *E. coli*; nutrition competition had a key role in resistance. *K. michiganensis* also delayed colonization of the pathogen *Salmonella enterica* serovar Typhimurium, prolonging host survival. A shared microbial reservoir is therefore critical for maintaining colonization resistance against invading microorganisms.

Results

Singly housed mice respond more heterogeneously to streptomycin than co-housed mice. We previously observed that the effect of antibiotics on gut microbiota composition varied among singly housed mice[24]. As mice are coprophagic and co-housing is used to reduce variability among animals before experiments[38,39], we studied the effect of housing strategy during and after antibiotics treatment to determine whether exchange of microbiota members due to co-housing has functional consequences on properties such as colonization resistance. To achieve this, we studied microbiota composition in four independent cohorts of sibling mice during and after streptomycin treatment; each cohort was split into co-housed and singly housed groups (Fig. 1a).

Sequencing of microbiota 16S revealed that the samples that were collected before treatment with streptomycin mainly consisted of the two major phyla found in mammalian guts—Bacteroidetes (~70%) and Firmicutes (~20%; Extended Data Fig. 1a,b). Other

[1]Instituto Gulbenkian de Ciência, Oeiras, Portugal. [2]Department of Bioengineering, Stanford University School of Medicine, Stanford, CA, USA. [3]Department of Microbiology & Immunology, Stanford University School of Medicine, Stanford, CA, USA. [4]Chan Zuckerberg Biohub, San Francisco, CA, USA. *e-mail: kxavier@igc.gulbenkian.pt

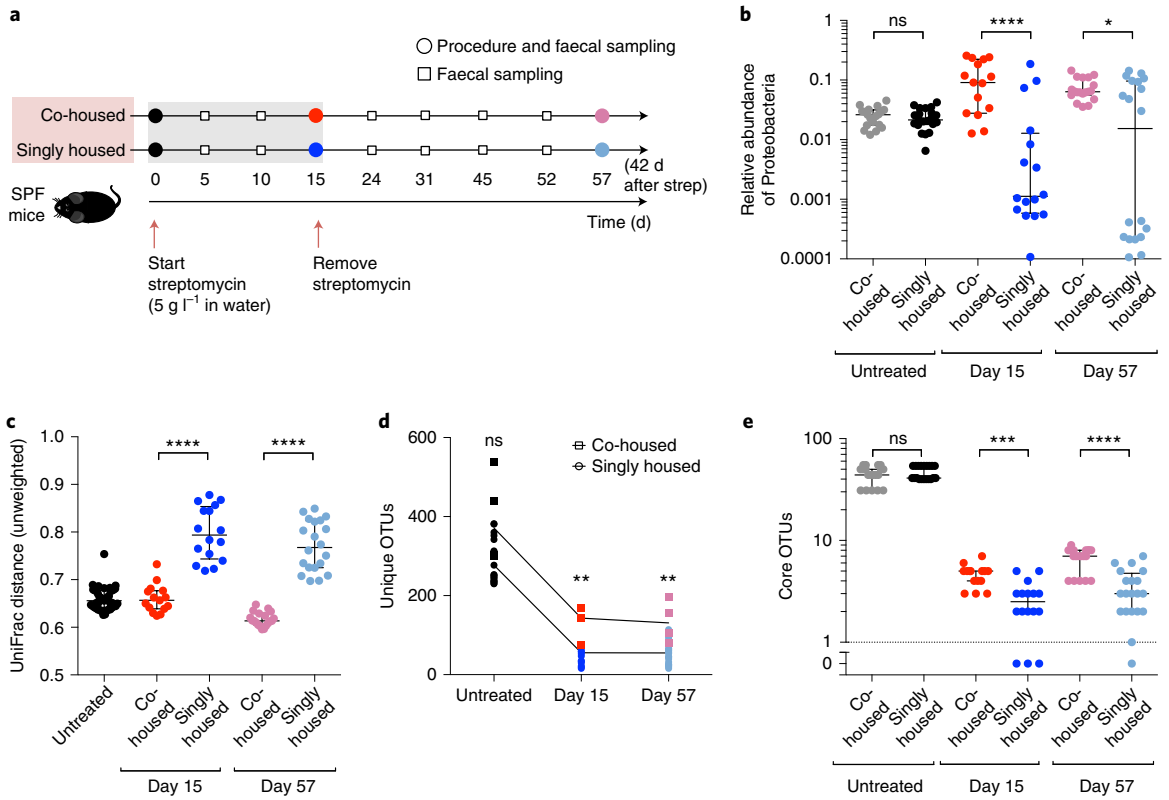

Fig. 1 | Streptomycin causes stochastic changes in the microbiota composition and a decrease in diversity in singly housed mice compared with co-housed mice. a, Experimental scheme of before and after treatment with streptomycin (strep) in four independent mice cohorts (10–11 mice in each). Streptomycin (5 g l^{-1}) was administered in the drinking water to 5 co-housed and 5–6 singly housed specific-pathogen-free (SPF) C57BL/6J mice on day 0 and removed on day 15. Faecal samples were collected before (day 0), during (day 15) and after (day 57) antibiotics treatment for microbiota composition analysis. Procedures (circles) denote the start (day 0) or end (day 15) of streptomycin treatment and the time of euthanasia (day 57). **b**, Relative abundances of the Proteobacteria phylum in co-housed and singly housed mice at the indicated time points. **c**, Phylogenetic dissimilarities on each day determined by the mean unweighted UniFrac distance of the bacterial communities of each mouse to each other mouse within the same group. **d**, Gamma-diversity of the gut microbiota of the co-housed and singly housed mice at the indicated time points. **e**, Number of core OTUs present in every mouse of each group at days 0 (before treatment), 15 and 57. For **b**,**c**,**e**, data are median ± interquartile ranges, representing $n = 20$ (day 0), $n = 15$ (day 15) and $n = 19$ (day 57) co-housed and $n = 21$ (day 0), $n = 16$ (day 15) and $n = 20$ (day 57) singly housed mice from 4 (days 0 and 57) or 3 (day 15) independent experiments. For **d**, data are median, representing $n = 4$ cages (days 0 and 57) or $n = 3$ cages (day 15) of co-housed mice, and $n = 21$ (day 0), $n = 16$ (day 15) and $n = 20$ (day 57) singly housed mice from 4 (days 0 and 57) or 3 (day 15) independent experiments. For **b**–**e**, statistical analysis was performed using two-tailed Mann–Whitney *U*-tests; $^{*}P < 0.05$, $^{***}P < 0.001$, $^{****}P < 0.0001$; ns, not significant.

phyla accounted for less than 10% of total abundance on average (Fig. 1b, Proteobacteria; Extended Data Fig. 1c, Verrucomicrobia). After 15 d of treatment, the abundances of Bacteroidetes and Firmicutes were extremely variable in singly housed mice compared with the abundances in co-housed and untreated mice (Extended Data Fig. 1a,b). The Proteobacteria phylum increased in most co-housed mice during treatment (Fig. 1b); by contrast, in most singly housed mice, Proteobacteria decreased to very low levels. After treatment with streptomycin, Proteobacteria continued to differ substantially between the two groups—Proteobacteria were maintained at high levels in all of the co-housed mice, but recovered in only 10 out of 20 singly housed mice (Fig. 1b). These findings highlight the potential for increased microbial extinction in singly housed mice.

UniFrac distances between all of the sample pairs within each group of each cohort at different time points, a measure of compositional dissimilarity, were significantly lower in the microbiotas of co-housed mice during and after antibiotics treatment compared with singly housed mice (Fig. 1c), indicating that co-housed mice have higher microbiota homogeneity than singly housed mice.

To quantify the environmental bacterial reservoir across housing conditions, we calculated the gamma-diversity for co-housed mice and for each singly housed mouse. During and after streptomycin treatment, gamma-diversity was higher in co-housed mice than in any of the singly housed mice (Fig. 1d). Furthermore, singly housed mice lost significantly more core operational taxonomic units (OTUs) due to treatment (see Methods) than co-housed mice, confirming that co-housed mice maintained a more diverse environmental microbial reservoir (Fig. 1e, Extended Data Fig. 1d).

We also tested the effect of housing in response to treatment with ciprofloxacin—an antibiotic with a different mechanism of action. We observed that ciprofloxacin and streptomycin elicited similar compositional and diversity signatures distinguishing co-housed and singly housed microbiota responses after treatment (Extended Data Fig. 2; Supplementary Discussion). Overall, these data demonstrate that cohabiting mice have a more homogeneous microbiota and preserve larger bacterial reservoirs during and after antibiotics treatment compared with singly housed mice, which experience eradication of subsets of species that vary across individuals.

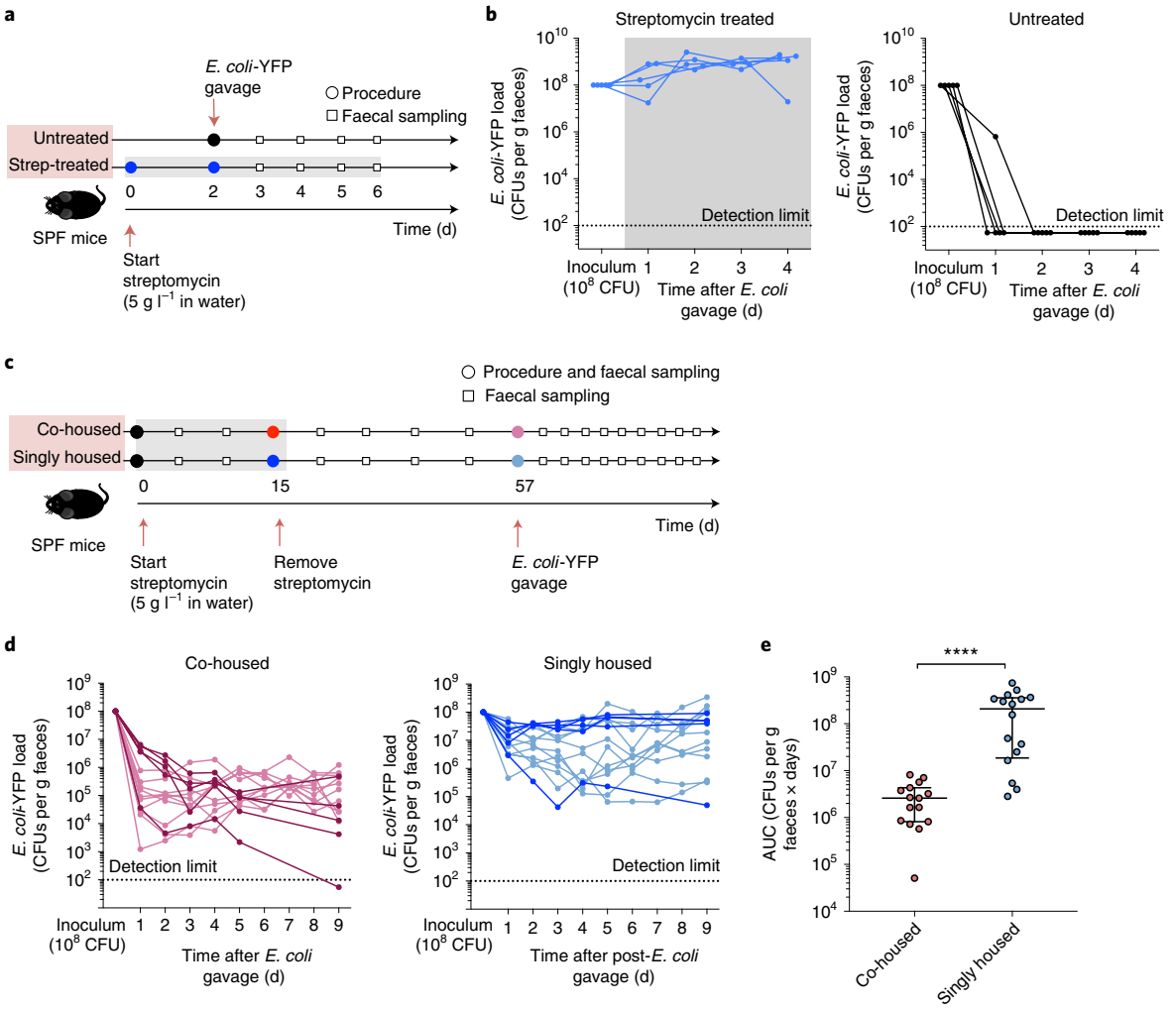

Fig. 2 | Co-housed mice are resistant to *E. coli* colonization, in contrast to most singly housed mice. a, Experimental scheme for measuring the ability of mice to resist colonization by *E. coli*. *E. coli*-YFP cells were orally administered to cohorts of untreated and streptomycin-treated mice on day 2. Faecal samples were collected at the indicated time points for *E. coli*-YFP quantification. Procedures (circles) denote start of streptomycin treatment (day 0) and gavage with *E. coli*-YFP (day 2). **b**, Loads of *E. coli*-YFP (CFUs per g faeces) remained high in streptomycin-treated mice (left; grey shading indicates streptomycin treatment), but became undetectable in untreated mice by day 1–2 (right); $n = 5$ mice per group. **c**, Experimental scheme for measuring the ability of mice to resist colonization by *E. coli* in 3 out of the 4 independent cohorts of co-housed and singly housed mice after streptomycin treatment. *E. coli*-YFP cells were orally administered to all of the mice on day 57. Faecal samples were collected for 9 days after gavage for *E. coli*-YFP quantification. Procedures (circles) denote the start (day 0) or end (day 15) of streptomycin treatment and time of gavage with *E. coli*-YFP (day 57). **d**, Loads of *E. coli*-YFP colonization in cohorts 2–4 in co-housed mice (left) and singly housed mice (right); $n = 15$–16 mice per group from three independent experiments; all of the experiments exhibited similar results. Loads of *E. coli*-YFP in cohort 2 are shown in dark pink or dark blue. In this cohort, the loads of *E. coli*-YFP gradually decreased in co-housed mice (dark pink lines; left), but remained high in all of the singly housed mice except for mouse 10 (dark blue lines, right). The microbiota composition of cohort 2 was analysed in samples from days 0, 15 and 57 of co-housed (mouse 1–5) and singly housed (mouse 6–10) mice (Extended Data Fig. 3); $n = 5$ mice per group in cohort 2. **e**, AUC calculated from the dynamics of *E. coli*-YFP CFUs per g faeces during the experiment for each of the co-housed and singly housed mice of the 3 cohorts tested in **d**, demonstrating that co-housed mice had significantly lower loads of *E. coli* throughout the experiment than singly housed mice; $n = 15$–16 mice per group from three independent experiments; all of the experiments exhibited similar results. For **e**, data are median ± interquartile range; statistical analysis was performed using two-tailed Mann–Whitney *U*-tests.

The heterogeneous impact of antibiotics in singly housed mice leads to lower colonization resistance against *E. coli*. We hypothesized that the microbiota heterogeneity in antibiotic-treated singly housed mice might have functional implications, such as variable colonization-resistance capacity. Certain Proteobacteria, such as *E. coli*, have been shown to colonize mammalian hosts better after streptomycin treatment[19,24,40,41]; indeed, streptomycin-resistant *E. coli* labelled with yellow fluorescent protein (YFP) robustly colonized singly housed mice after streptomycin treatment (Fig. 2a,b, left). *E. coli* loads in faecal samples were around 10^8 colony-forming units (CFUs) per g 1 d after gavage and maintained or increased thereafter (Fig. 2b, left). By contrast, untreated mice were fully resistant to invasion, with *E. coli*-YFP at undetectable levels after day 1 (Fig. 2b, right). The microbiotas of untreated mice were therefore highly resistant to *E. coli* colonization, as reported previously[15,19,40], validating this model to use colonization-resistance capacity as a measurement of the functional potential of microbiotas.

To examine the functional consequence of single housing, after streptomycin treatment, we challenged all of the mice from three of the initial cohorts described in Fig. 1 with *E. coli* (Fig. 2c). Overall,

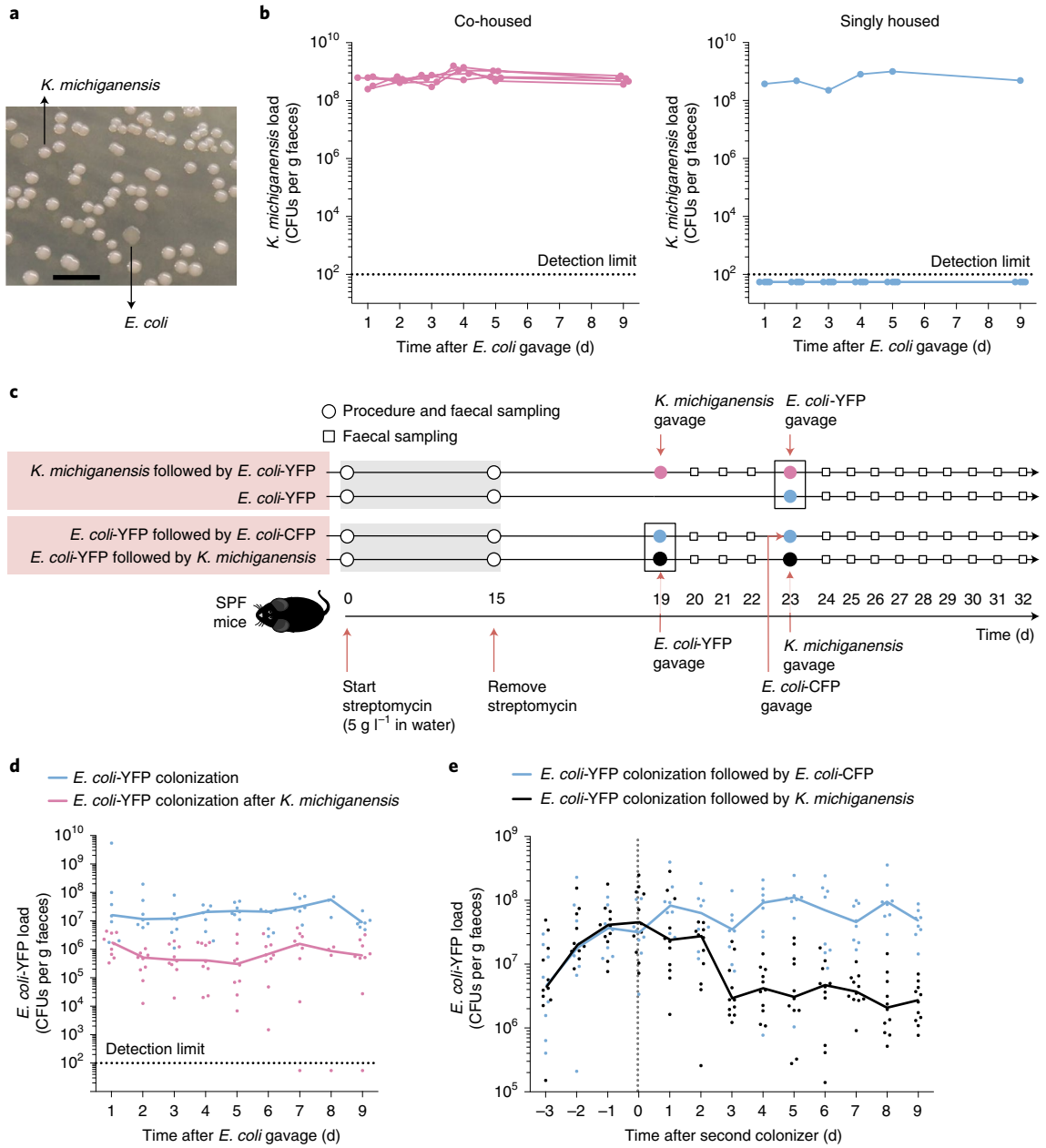

Fig. 3 | *K. michiganensis* provides colonization resistance against *E. coli*. **a**, *E. coli* and *K. michiganensis* are easily distinguishable on the basis of colony morphology when grown on LB agar and incubated overnight at 37 °C. Similar results were obtained in two independent experiments. Scale bar, 0.5 cm. **b**, After streptomycin treatment, loads of *K. michiganensis* (CFUs per g faeces) in mice from cohort 2 of the experiment shown in Fig. 2c,d were high in co-housed mice (left) but at undetectable levels in all of the singly housed mice except one (right); $n = 5$ mice per group. **c**, Experimental scheme for measuring the ability of singly housed mice associated with *K. michiganensis* to increase colonization resistance against or displace *E. coli* after streptomycin treatment. Streptomycin (5 g l^{-1}) was administered in the drinking water starting on day 0 and removed on day 15. Faecal samples were collected before (day 0), during (day 15) and after (days 19, 23, 28 and 32) treatment with antibiotics. *K. michiganensis*, *E. coli*-YFP or *E. coli*-CFP cells were orally administered on the indicated days. Faecal samples were collected daily after gavage for *K. michiganensis* and *E. coli* quantification. Procedures (circles) denote the start (day 0) or end (day 15) of streptomycin treatment and gavage with *E. coli*-YFP, *E. coli*-CFP or *K. michiganensis* (days 19 or 23). **d**, Loads of *E. coli*-YFP (CFUs per g faeces) when colonizing mice in the absence of *K. michiganensis* were higher than in mice precolonized with *K. michiganensis*; $n = 7$ mice (*E. coli*-YFP group) and $n = 9$ mice (*K. michiganensis* + *E. coli*-YFP group) across two independent experiments, which yielded similar results; AUC comparisons are provided in Extended Data Fig. 4b. **e**, *E. coli*-YFP (CFUs per g faeces) colonization before and after challenge with *E. coli*-CFP ($n = 8$ across two independent experiments, which yielded similar results) or *K. michiganensis* ($n = 11$ across three independent experiments, which yielded similar results). *K. michiganensis* gavage resulted in a substantial decrease in *E. coli* loads. AUC comparisons are provided in Extended Data Fig. 4d. For **d**,**e**, data are median; the circles represent values from individual mice.

co-housed mice had lower loads of *E. coli*-YFP than singly housed mice (Fig. 2d). We calculated the area under the curve (AUC) for the dynamics of *E. coli*-YFP CFUs per g and found that co-housed mice had significantly lower *E. coli* loads throughout compared with the loads of singly housed mice (Fig. 2e). Interestingly, a small number of singly housed mice behaved similarly to co-housed mice.

This bimodal behaviour was particularly stark in cohort 2 (Fig. 2d, dark pink and dark blue lines), in which one singly housed mouse (mouse 10) exhibited a 1,000-fold decrease in *E. coli*-YFP loads in comparison to the other singly housed mice. In this cohort, *E. coli* loads dropped steadily after gavage in all of the co-housed mice, ranging from around 10^6 CFUs per g to undetectable on day 9 (Fig. 2d, dark pink lines). Only singly housed mouse 10 exhibited decrease kinetics of *E. coli* loads that were similar to those of co-housed mice; all of the other singly housed mice maintained high levels throughout (Fig. 2d, dark blue lines). Thus, after streptomycin treatment, the maintenance of colonization resistance to *E. coli* is highly dependent on housing and is heterogeneous across singly housed mice.

***K. michiganensis* is sufficient to provide colonization resistance in antibiotic-treated mice**. Although most of the singly housed mice were susceptible to *E. coli* colonization, we were intrigued by the mouse from cohort 2 that behaved like the co-housed mice (Fig. 2d). After plating on Luria–Bertani (LB) agar, samples from this mouse exhibited a high number of non-YFP colonies with different morphology from *E. coli* (Fig. 3a). These streptomycin-sensitive non-YFP colonies were present in all of the co-housed samples of cohort 2, but were present only in mouse 10 among the singly housed mice (Fig. 3b). 16S rRNA Sanger sequencing revealed that these colonies were *Klebsiella* spp. We next analysed the microbiota composition that was present before *E. coli* gavage (Extended Data Fig. 3a). To identify species that could confer colonization resistance against *E. coli*, we compared the microbiota of mice exhibiting colonization resistance against *E. coli* (all of the co-housed mice (1–5), and singly housed mouse 10) with the 4 singly housed mice that were susceptible to *E. coli* colonization. Using the linear discriminant analysis effect size (LEfSe)[42] method, we identified 2 OTUs associated with no colonization resistance, and 5 OTUs associated with colonization resistance (Extended Data Fig. 3b–d). Interestingly, only *Klebsiella* (OTU 8) was both undetectable in all of the mice susceptible to *E. coli* and present in all of the colonization-resistant mice (Extended Data Fig. 3d). Moreover, *Klebsiella*-associated mice had significantly lower levels of *E. coli*-YFP compared with the non-*Klebsiella*-associated mice from cohort 2 (Extended Data Fig. 3e). We found that *Klebsiella* spp. were low abundance members (below the detection limit of 16S sequencing) of only a fraction of normal mouse microbiotas (Supplementary Table 1, Supplementary Discussion), and their survival after antibiotics treatment was highly susceptible to housing. Proteobacteria often go extinct after streptomycin treatment in singly housed mice; however, when present in co-housed mice, Proteobacteria were maintained in every mouse within the same cage (Supplementary Fig. 1). Whole-genome sequencing of *Klebsiella* clones from cohort 2 revealed that this species is *K. michiganensis*, a close relative of *Klebsiella oxytoca*[43] that lacks the pathogenicity of other *Klebsiella* spp.[43].

To test whether *K. michiganensis* isolates were sufficient for colonization resistance in singly housed mice, we repeated the streptomycin-treatment experiment with a reduced post-antibiotic period, and challenged mice with *E. coli*-YFP; a subset of the mice were preassociated with *K. michiganensis* (Fig. 3c). In mice that were not gavaged with *K. michiganensis*, *E. coli*-YFP CFUs remained high throughout (Fig. 3d). By contrast, in all of the mice gavaged with *K. michiganensis, K. michiganensis* loads remained unchanged, whereas *E. coli*-YFP loads were significantly lower by 10-fold to 100-fold (Fig. 3d, Extended Data Fig. 4a,b).

To determine whether *E. coli* loads were dependent on which species arrived first in the gut, we tested displacement of *E. coli* by challenging mice that were precolonized with *E. coli*-YFP with 10^8 CFUs of either *K. michiganensis* or *E. coli*-CFP as a control (Fig. 3c). Then, 4 d after *E. coli*-YFP gavage, all of the mice were colonized with *E. coli*-YFP at approximately 10^7 CFUs per g (Fig. 3e). As expected, in mice gavaged with *E. coli*-CFP, *E. coli*-YFP loads remained high (10^7–10^8 CFUs per g; Fig. 3e) and *E. coli*-CFP could colonize at only 10^3–10^4 CFUs per g because the gut was already occupied by the isogenic *E. coli*-YFP strain (Extended Data Fig. 4c). By contrast, after introduction of *K. michiganensis*, *E. coli*-YFP loads decreased significantly over the first 3 d and stabilized at around 10^6 CFUs per g (Fig. 3e; Extended Data Fig. 4d, AUC), whereas *K. michiganensis* loads increased to approximately 10^9 and remained high thereafter (Extended Data Fig. 4c). Our data therefore indicate that *K. michiganensis* is sufficient for colonization resistance to *E. coli* under streptomycin-induced disruption, independent of colonization order.

***K. michiganensis* outcompetes *E. coli* through nutrition competition**. To gain insights into the mechanism by which *K. michiganensis* impairs *E. coli* colonization, we tested whether they occupy similar spatial locations by imaging gut sections from mice receiving both *E. coli* and *K. michiganensis*. *E. coli* was often found in the same region as, albeit not in close proximity to, *K. michiganensis* (Fig. 4a). In fact, both Gammaproteobacteria appeared to be spread out within the lumen, suggesting that they share similar niches and are therefore likely to compete directly for nutrients.

To test whether nutrition competition could explain the advantage of *K. michiganensis* over *E. coli* in vivo, we quantified in vitro growth in LB medium of monocultures of *E. coli*-YFP and *K. michiganensis* and co-cultures of *E. coli*-YFP with either *K. michiganensis* or *E. coli*-CFP. All of the cultures initially grew with similar dynamics; the mono- and co-cultures containing *K. michiganensis* achieved higher yields, whereas the co-culture of *E. coli*-YFP + *E. coli*-CFP grew indistinguishably from *E. coli*-YFP alone (Fig. 4b). YFP levels in the *E. coli*-YFP + *K. michiganensis* co-cultures diverged from the YFP levels in the *E. coli*-YFP + *E. coli*-CFP co-cultures after 7 h and remained lower thereafter (Fig. 4c), suggesting that *K. michiganensis* has a competitive advantage.

As LB provides a rich environment for Enterobacteriaceae, we hypothesized that *K. michiganensis* has a greater fitness advantage under nutrient-limited conditions. We therefore tested growth in minimal medium with one of several simple sugars that both species can consume in isolation, including dietary-based sugars (fructose, glucose, arabinose and xylose)[44,45] or a mucus-layer-derived simple sugar (fucose)[45]. Across all of the carbon sources, cultures with *K. michiganensis* had higher growth rates and achieved higher yields than monocultures of *E. coli* (Fig. 4d). *E. coli*-YFP + *K. michiganensis* co-cultures grew with similar dynamics as *K. michiganensis* monocultures (Fig. 4d), but YFP levels in *E. coli*-YFP + *K. michiganensis* co-cultures were substantially lower than in *E. coli*-YFP + *E. coli*-CFP co-cultures (Fig. 4e). Thus, *K. michiganensis* effectively outcompetes *E. coli* in all of the carbon-source conditions tested.

These bulk growth experiments do not exclude models on the basis of physical interaction or chemical warfare between the two species. However, our tests of several competition strategies provide evidence against the killing of *E. coli* or inhibition either by a contact-dependent mechanism or by inhibitory compounds produced by *K. michiganensis* (Extended Data Fig. 5, Supplementary Discussion). Instead, the general growth advantage of *K. michiganensis* over *E. coli* is the probable explanation for reduced *E. coli* abundance in hosts containing *K. michiganensis*.

An *E. coli*-exclusive carbon source delays the colonization-resistance capacity of *K. michiganensis* in vivo. To test whether nutrient competition drives gut interactions between *E. coli* and *K. michiganensis*, we hypothesized that in vivo colonization of *E. coli* is facilitated by a nutritional advantage through addition of a carbon source that is accessible to *E. coli* but not to *K. michiganensis*, such as galactitol[46] (Extended Data Fig. 6a). To test this hypothesis, we repeated the displacement experiment above, supplementing the

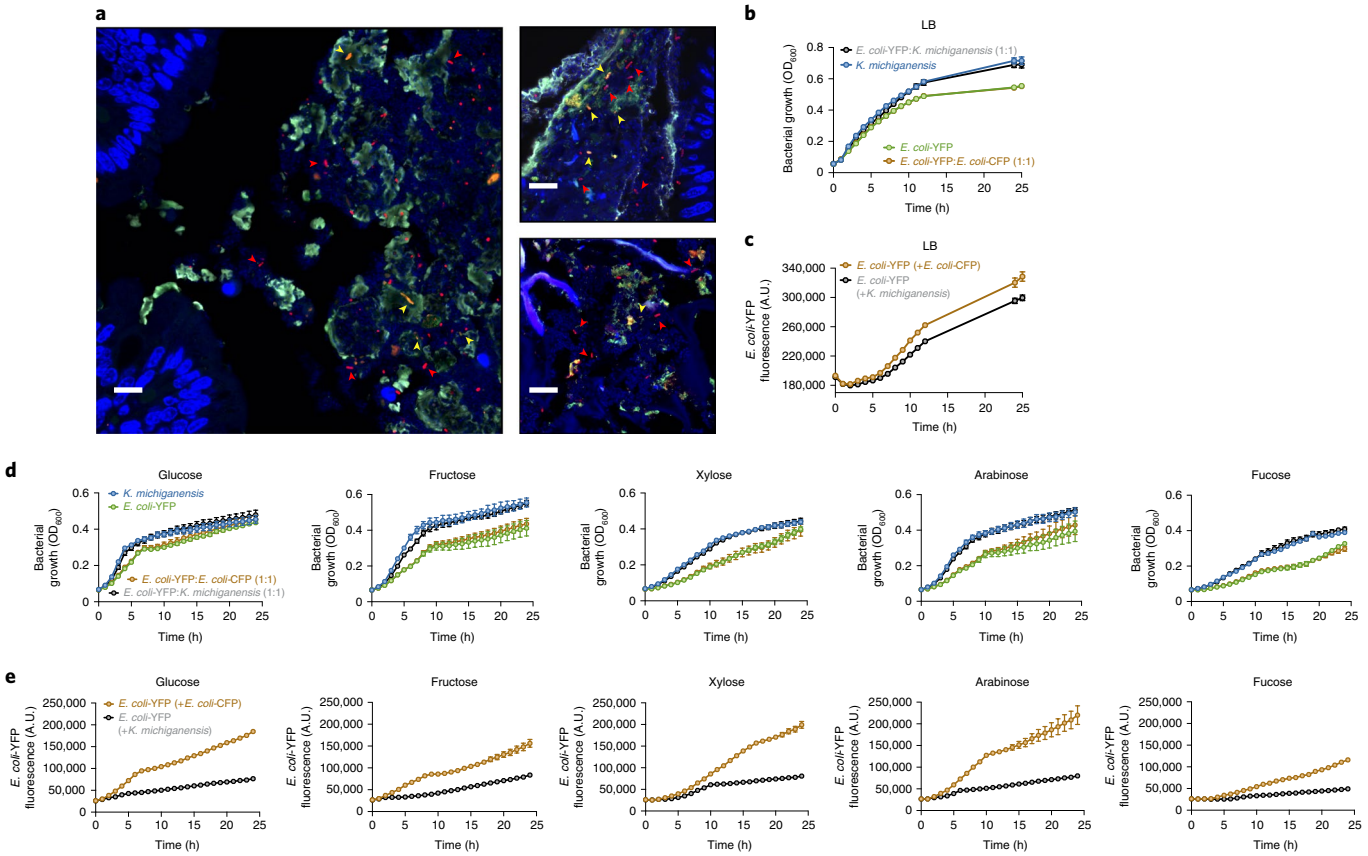

Fig. 4 | Competition for simple sugars provides a fitness advantage to *K. michiganensis* over *E. coli*. **a**, Intestinal sections were stained with 16S rRNA fluorescence in situ hybridization (FISH) probes targeting Gammaproteobacteria (red) and *E. coli* (green). In the images, *E. coli* (yellow; cells are targeted with both red and green FISH probes) and *K. michiganensis* (red; targeted with only the Gammaproteobacteria probe) were in close proximity in many regions of the colon of mice colonized with both species, indicating that they inhabited similar spatial niches. Mucus (green) and DNA (blue) were stained with UEA1 and DAPI, respectively. The large, puffy diffuse green staining is mucus. There were no bacteria-sized objects that appeared in only the green channel; all such green-stained objects were also red stained and therefore appeared yellow. Scale bars, 10 µm. Data are from one experiment. **b**, The cell density of co-cultures of *E. coli*-YFP with *K. michiganensis* or *E. coli*-CFP showed that *K. michiganensis* has a slight advantage in LB medium. Growth was monitored by optical density at 600 nm (OD_{600}) measurements; $n = 3$ technical replicates per condition. **c**, The growth ability of *E. coli*-YFP in LB medium was lower in co-cultures with *K. michiganensis* as compared with *E. coli*-CFP. *E. coli*-YFP growth was monitored by quantification of YFP fluorescence; $n = 3$ technical replicates per condition. **d**, The sugar-utilization capacity of *K. michiganensis* and *E. coli* alone or in co-cultures in minimal medium containing 0.25% of the indicated carbon source. Growth was monitored by OD_{600} measurements every hour for 24 h; $n = 6$ technical replicates curves per condition. *K. michiganensis* generally exhibited faster growth than *E. coli* across all of the carbon sources. **e**, *E. coli*-YFP growth ability in co-cultures in minimal medium containing 0.25% of the indicated carbon source. *E. coli*-YFP growth was monitored by quantification of YFP fluorescence every hour for 24 h; $n = 6$ technical replicates per condition. *E. coli* yield was lower when grown with *K. michiganensis* compared with *E. coli*-CFP, across all of the carbon sources. For **b**–**e**, data are mean ± s.d.

water with 2% galactitol (Fig. 5a). Then, 1 d after *E. coli*-YFP gavage, *E. coli*-YFP levels were around 10^7 CFUs per g, and remained at 10^7–10^8 CFUs per g thereafter. After *K. michiganensis* gavage, *E. coli*-YFP loads slowly decreased in mice drinking galactitol, reaching 10^6 after only 6 d (Fig. 5b). These data differed substantially from our previous experiments, in which *K. michiganensis* in mice drinking non-supplemented water caused *E. coli*-YFP to drop from 10^8 to 10^6 CFUs per g after 3 d (Fig. 5b; Extended Data Fig. 6d, AUC). *K. michiganensis* levels were high throughout regardless of *E. coli*-YFP loads and galactitol (Extended Data Fig. 6c). Thus, galactitol staved off colonization resistance to *E. coli* for 3 d.

We reasoned that the transient effect of galactitol could be due to its consumption by other microorganisms, the proliferation of which attenuated the nutritional advantage of *E. coli* over time. To test whether we could prolong the *E. coli* nutritional advantage over *K. michiganensis* due to galactitol without interference from other microorganisms, we compared the colonization-resistance capacity of *K. michiganensis* with that of *E. coli* in bi-colonized gnotobiotic mice with or without galactitol in the water. As a control, we also tested *K. michiganensis* against a Δ*gatZ E. coli* mutant that is unable to consume galactitol (Fig. 5c). These experiments also tested whether *K. michiganensis* can establish colonization resistance to *E. coli* in the gut in the absence of other species. One day after *E. coli*-YFP gavage, *E. coli*-YFP levels were around 10^8 CFUs per g in the group with non-supplemented water, increasing to approximately 10^9 CFUs per g after 4 d. After *K. michiganensis* gavage, *E. coli*-YFP loads decreased immediately, dropping 1,000-fold in 2 d and remaining at 10^6–10^7 CFUs per g thereafter (Fig. 5d). By contrast, in mice colonized with *E. coli*-YFP in the galactitol-supplemented-water condition, *E. coli*-YFP levels were already higher on day −3 (10^8–10^{10} CFUs per g), stabilizing at approximately 10^9 CFUs per g in 4 d. After *K. michiganensis* gavage, *E. coli*-YFP loads decreased slightly in the first 2 d to around 10^8 CFUs per g, but stabilized thereafter, at significantly higher (10-fold to 100-fold) loads compared with the loads in mice drinking non-supplemented water (Fig. 5d; Extended Data Fig. 6f, AUC). The control group that was gavaged

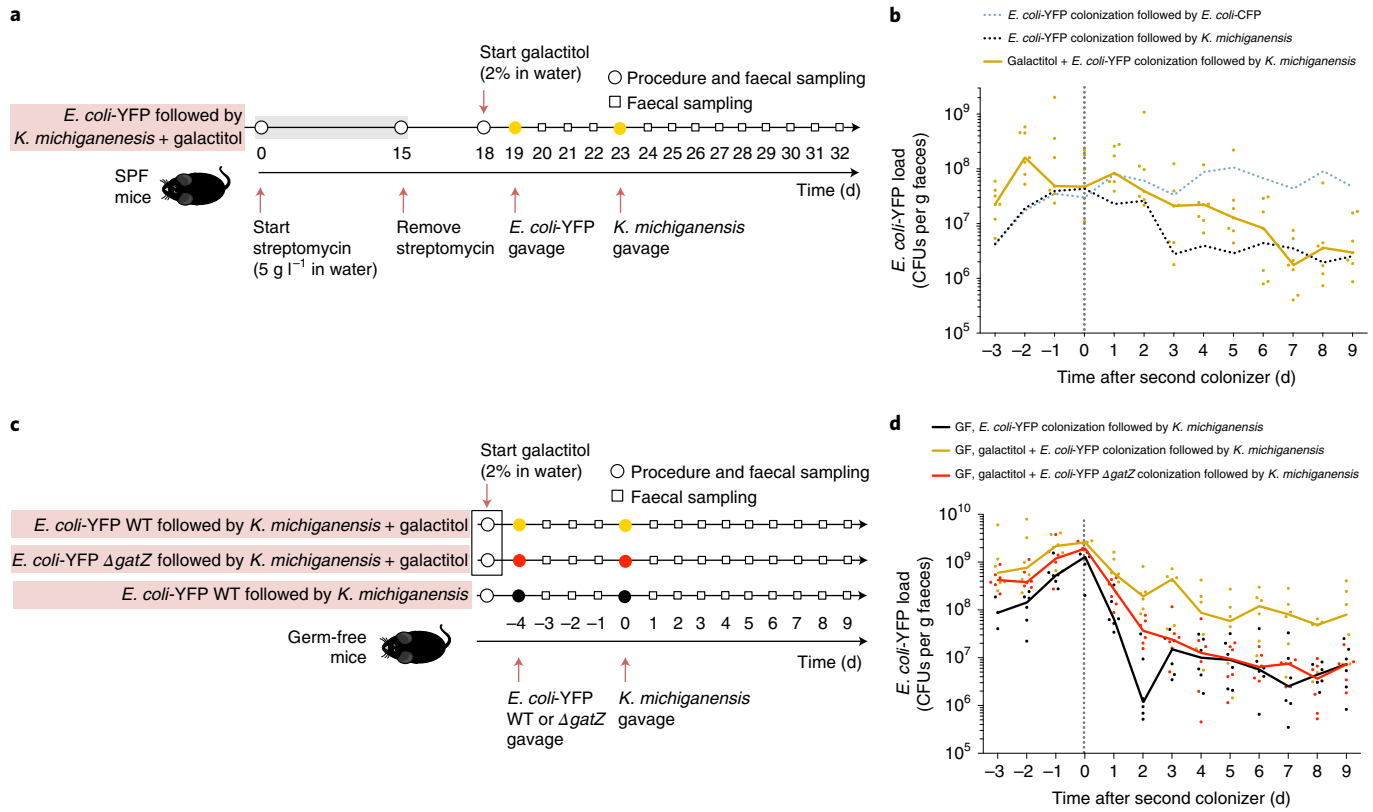

Fig. 5 | A nutritional advantage for *E. coli* abolishes the colonization-resistance capacity of *K. michiganensis*. **a**, Experimental scheme for measuring the effect of galactitol on *K. michiganensis*-mediated colonization resistance against *E. coli* in singly housed mice after treatment with streptomycin. Streptomycin (5 g l^{-1}) was administered in the drinking water from day 0 to day 15. Faecal samples were collected before (day 0), during (day 15) and after (days 19, 23, 28 and 32) treatment with antibiotics. The mice were given water supplemented with 2% galactitol from day 18 onwards. *K. michiganensis* or *E. coli*-YFP cells were orally administered on the indicated days. Faecal samples were collected daily after gavage for *K. michiganensis* and *E. coli*-YFP quantification; $n = 7$ mice. Procedures (circles) denote the start (day 0) or end (day 15) of streptomycin treatment, start of galactitol-supplemented water (day 18), or gavage with *E. coli*-YFP or *K. michiganensis* (days 19 or 23, respectively). **b**, Loads of *E. coli*-YFP (CFUs per g faeces) before and after challenge with *K. michiganensis* in mice with drinking water supplemented with 2% galactitol (yellow dots and line); $n = 7$ mice across two independent experiments. The dashed lines represent median values of CFUs per g faeces of *E. coli*-YFP colonization before and after challenge with *E. coli*-CFP (blue) or *K. michiganensis* (black) in mice without galactitol administration from Fig. 3e. The experiments in Fig. 3e were performed in parallel with the groups from the two independent experiments that received galactitol, which are shown here for comparison. Galactitol attenuated the colonization resistance against *E. coli*. **c**, Experimental scheme for measuring the effect of galactitol on *K. michiganensis*-mediated colonization resistance against *E. coli* in singly housed gnotobiotic mice. Germ-free mice were given either non-supplemented water or water supplemented with 2% galactitol. *K. michiganensis*, *E. coli*-YFP or *E. coli*-YFP Δ*gatZ* cells were orally administered on the indicated days. Faecal samples were collected daily after gavage for *K. michiganensis*, *E. coli*-YFP and *E. coli*-YFP Δ*gatZ* quantification; $n = 6$ mice across two independent experiments. Procedures (circles) denote the start of galactitol-supplemented water (day −5), gavage with *E. coli*-YFP WT or Δ*gatZ* (day −4) or gavage with *K. michiganensis* (day 0). **d**, Loads of *E. coli*-YFP and *E. coli*-YFP Δ*gatZ* (CFUs per g faeces) before and after challenge with *K. michiganensis* in mice with non-supplemented drinking water or water supplemented with 2% galactitol; $n = 6$ mice across two independent experiments. Galactitol attenuated the colonization resistance against *E. coli* in mice that were previously germ-free (GF). Data are median; the circles represent values from individual mice. For **b**,**d**, AUC comparisons are provided in Extended Data Fig. 6d,f, respectively.

with Δ*gatZ E. coli*-YFP colonized to similar levels as *E. coli*-YFP in the initial 4 d under galactitol supplementation (Fig. 5d), despite its inability to consume galactitol; this lack of fitness change was unsurprising because Δ*gatZ E. coli* is known to have higher fitness in mouse gut colonization compared with wild-type *E. coli*[47]. After *K. michiganensis* gavage, Δ*gatZ E. coli*-YFP loads decreased immediately, dropping 100-fold in 2 d and remaining at 10^6–10^7 CFUs per g thereafter (Fig. 5d), similar to wild-type *E. coli*-YFP without galactitol (Extended Data Fig. 6f). Overall, these data show that *K. michiganensis* can directly establish colonization resistance to *E. coli* in the gut. Moreover, without other microorganisms, a nutritional advantage to *E. coli* abolishes colonization resistance by *K. michiganensis*, enabling both bacteria to colonize at high levels (Fig. 5d, Extended Data Fig. 6e), supporting nutrition competition as the mechanistic basis of colonization resistance.

***K. michiganensis* prolongs host survival after *Salmonella* infection.** We next tested whether *K. michiganensis* can provide colonization resistance to the enteric pathogen *S.* Typhimurium, an Enterobacteriaceae like *E. coli*. In vitro co-cultures of *K. michiganensis* and *S.* Typhimurium-mCherry in minimal medium with fructose or glucose showed that, after 9–10 h of growth, mCherry levels decreased compared with *S.* Typhimurium-mCherry co-cultured with unlabelled *S.* Typhimurium or a murine commensal *E. coli* (Extended Data Fig. 7a). In minimal medium with arabinose or fucose, mCherry levels in co-cultures of *S.* Typhimurium-mCherry and *K. michiganensis* decreased only slightly, and at a later growth stage (Extended Data Fig. 7a).

We then tested the colonization-resistance capacity *K. michiganensis* and commensal *E. coli* individually against *S.* Typhimurium in vivo (Fig. 6a). In the absence of *K. michiganensis*—independent

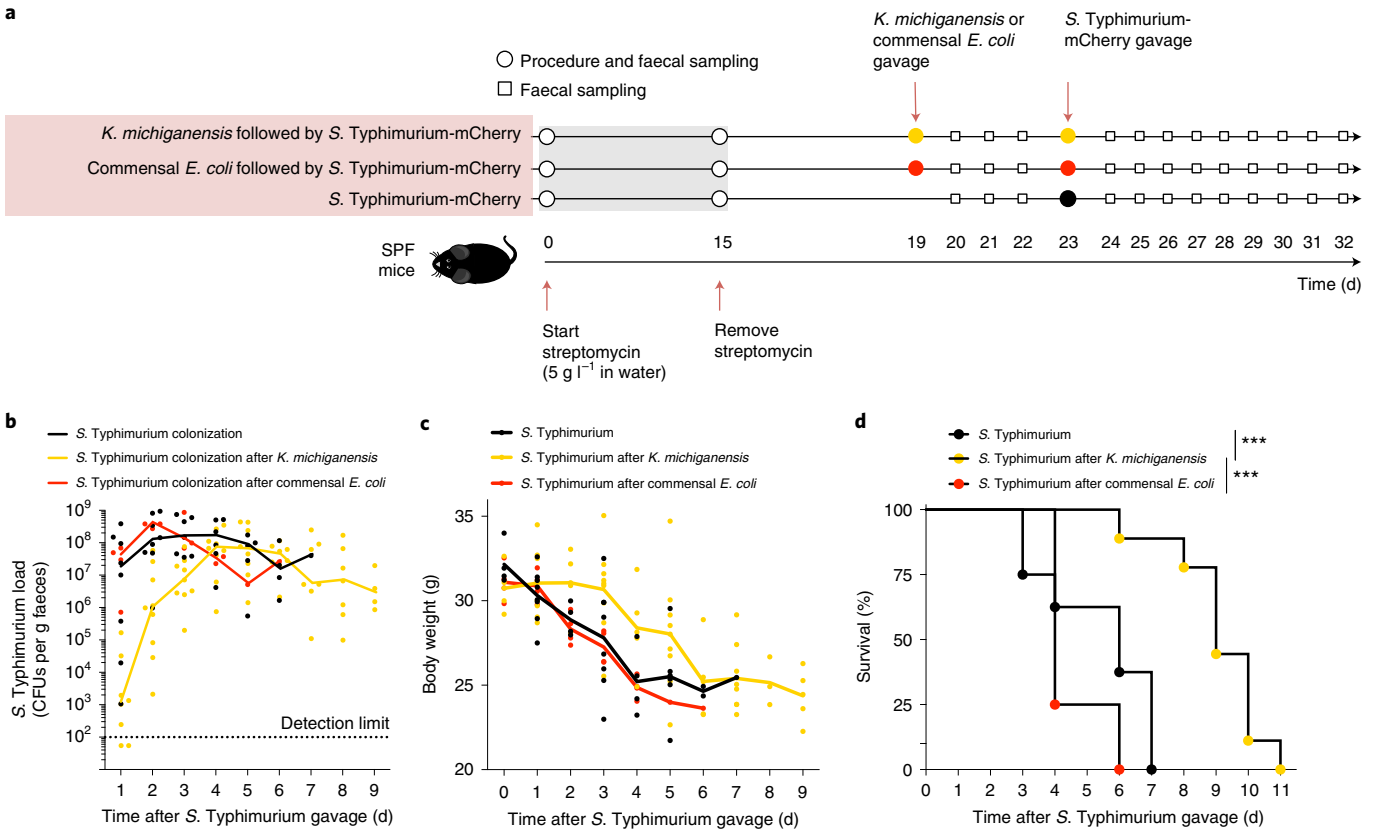

Fig. 6 | *K. michiganensis* delays gut expansion of *S.* Typhimurium. a, Experimental scheme for measuring the ability of singly housed mice to resist colonization by *S.* Typhimurium after treatment with streptomycin. Streptomycin was administered in the drinking water, starting on day 0 and ending on day 15. Faecal samples were collected before (day 0) and at the end (day 15) of treatment with antibiotics and daily on days 19–32. *K. michiganensis*, commensal *E. coli* and *S.* Typhimurium were orally administered on the indicated days. Faecal samples were collected daily after gavage for *K. michiganensis*, commensal *E. coli* and *S.* Typhimurium quantification. Procedures (circles) denote the start (day 0) or end (day 15) of streptomycin treatment, gavage with commensal *E. coli* or *K. michiganensis* (day 19), or gavage with *S.* Typhimurium (day 23). **b**, Loads of *S.* Typhimurium (CFUs per g faeces) increased more slowly in mice that were precolonized with *K. michiganensis* ($n=9$ mice across two independent experiments) compared with mice that either were not or were precolonized with a commensal *E. coli* ($n=8$ mice across two independent experiments and $n=4$ mice in one experiment, respectively). **c**, Loss in body weight due to *S.* Typhimurium infection was delayed in mice that were precolonized with *K. michiganensis* ($n=9$ mice across two independent experiments) compared with mice that either were not or were precolonized with a commensal *E. coli* ($n=8$ mice across two independent experiments and $n=4$ mice in one experiment, respectively). **d**, Mice infected with *S.* Typhimurium exhibited extended survival when precolonized with *K. michiganensis* ($n=9$ mice across two independent experiments) compared with mice that either were not or were precolonized with a commensal *E. coli* ($n=8$ mice across two independent experiments and $n=4$ mice in one experiment, respectively). ***$P<0.001$. Statistical analysis was performed using log-rank (Mantel–Cox) tests. In **b**,**c**, data are median; the circles represent values from individual mice. For **b**, AUC comparisons are provided in Extended Data Fig. 7b.

of the presence of commensal *E. coli*—1 d after *S.* Typhimurium gavage, *S.* Typhimurium loads were around 10^7 CFUs per g, reaching approximately 10^8 CFUs per g by day 2–3 (Fig. 6b) and remaining high thereafter. By contrast, in mice with *K. michiganensis*, *S.* Typhimurium loads were significantly lower, and were barely detectable in 7 out of 9 mice on day 1, at 10^2–10^5 CFUs per g (Fig. 6b, Extended Data Fig. 7b). *S.* Typhimurium loads in all of these mice took 4–5 d to reach around 10^8 CFUs per g, stabilizing thereafter at 10^7–10^8 CFUs per g (Fig. 6b). *K. michiganensis* loads remained high throughout (Extended Data Fig. 7c). Overall, these results show that *K. michiganensis*, but not commensal *E. coli*, delays gut expansion of *S.* Typhimurium, staving off full colonization by 2 d.

Importantly, the *K. michiganensis*–*S.* Typhimurium interaction had a direct effect on the host, delaying both weight loss and mortality (Fig. 6c,d); *K. michiganensis* alone did not alter body weight (Extended Data Fig. 7d). With *K. michiganensis*, *S.* Typhimurium-infected mice survived 4–5 d longer than without. Interestingly, colonization resistance mediated by *K. michiganensis* impacted the expansion of *S.* Typhimurium during the growth period before *Salmonella*-induced inflammation remodelled the lumen[15] (before day 1). The different expansion kinetics of *S.* Typhimurium after day 1 with or without *K. michiganensis* suggest that the primary effect of *K. michiganensis* is on the initial pre-inflammation expansion of *S.* Typhimurium and not during acute inflammation. The observation that *K. michiganensis* has a protective effect in the absence of inflammation supports the idea that *K. michiganensis* engages in metabolic strategies to inhibit Enterobacteriaceae growth. This protective effect is not general to all other gut Enterobacteriaceae, as a commensal *E. coli* failed to protect mice. In summary, *K. michiganensis* altered the kinetics of *S.* Typhimurium infection by delaying colonization and postponing host mortality.

Discussion

Here, we show that co-housing is important for establishing and maintaining colonization resistance through antibiotic-induced perturbation. Stochastic loss of key protective gut commensals renders singly housed mice susceptible to enteric pathogens in the absence of environmental microbial reservoirs from other mice. It remains

unclear whether certain antibiotics are more protective of microorganisms that have a role in colonization resistance, motivating broader studies on how different antibiotics act on a common microbiota[37]. The effects are presumably dependent on the degree of perturbation, with higher doses and longer treatments likely to increase the probability of extinction. After streptomycin treatment, retaining *K. michiganensis* was sufficient to recover colonization resistance to *E. coli*; this was highlighted by the colonization resistance of the only singly housed mouse that retained *K. michiganensis*, emphasizing the functional importance of stochasticity during perturbations.

The colonization-resistance capacity of *K. michiganensis* is probably based on nutrient competition, as the provision of a nutritional advantage to *E. coli* delayed or mitigated resistance. Gut microbiota colonization resistance to enteric bacteria through nutrient competition has been previously proposed[48,49]; however, identification of microorganisms that are directly involved is still limited[4,16,50,51]. We showed that *K. michiganensis* can also confer colonization resistance to other Enterobacteriaceae, such as the pathogen *S.* Typhimurium; *K. michiganensis* staved off *S.* Typhimurium expansion and, more importantly, delayed host mortality. We suspect that this effect acts on the pre-inflammation period of infection, which could be potentiated in future studies given the recent reports that microbiota members affect other stages of *Salmonella* infection[21,52].

In humans, widespread antibiotic treatment leads to considerable long-term effects—some commensals have been eradicated from all hosts and are therefore unavailable for recolonization[53]. Species extinction is also exacerbated by other Western practices such as diet[11], laxatives[36] and hygiene, the latter being efficient at preventing infections but also at reducing microbiota diversity[54]. Despite obvious differences in behaviour that result in less microbial transmission among humans than in mice, sharing of environment also leads to more similar microbiotas in humans[40]. Furthermore, people living less sanitized lifestyles tend to share more microorganisms than their industrialized counterparts[55]. Our results therefore support the importance of microbiota sharing in human recovery from perturbations.

Faecal microbiota transplants and swabbing have been successful against *C. difficile* infections[56] and in the colonization of Caesarean-section newborns[57], respectively. However, donor selection for faecal microbiota transplants, which is critical for sensitive recipients, remains challenging owing to difficulties in defining healthy microbiotas. Identification of key species, such as *K. michiganensis*, that are responsible for relevant microbiota functions is of utmost importance for achieving robust recovery from perturbations. Our study raises the hope that for each potential pathogen there are related commensal microorganisms that are responsible for providing colonization resistance and/or pathogen displacement.

Our study demonstrates the importance of housing in stochastic extinction of key protective species, providing deeper understanding of interspecies interactions and mechanisms that drive colonization resistance. This knowledge should enable the design of strategies for the reacquisition of natural commensals and to routinely restore microbiota composition after antibiotics treatment[16]. Future therapies will probably involve personalized treatment and prophylaxis with defined bacterial cocktails with preferred prebiotics to tackle infections for each patient.

Methods

Animal experiments. All of the mouse experiments performed at Instituto Gulbenkian de Ciência (IGC) were approved by the Institutional Ethics Committee and the Portuguese National Entity (Direção Geral de Alimentação e Veterinária; 015190), which complies with European Directive 86/609/EEC of the European Council. All of the mouse experiments conducted at Stanford University were performed in accordance with the Administrative Panel on Laboratory Animal Care, Stanford University's IACUC.

C57BL/6J male mice were used at 6–8 weeks of age and were randomly assigned to experimental and control groups. C57BL/6J mice were used for all streptomycin and gnotobiology experiments. Swiss Webster male mice (aged 10 weeks) were used in the experiment with ciprofloxacin, and were randomly assigned to experimental and control groups. None of the animal experiments were performed blinded. Sample size was chosen according to institutional directives and in accordance with the guiding principles underpinning humane use of animals in research. No statistical analyses were performed to predetermine the sample sizes. All of the experiments were performed at least twice, with the exception of the in vivo experiment with commensal *E. coli* and the ciprofloxacin-treatment experiment, which were performed once.

Streptomycin treatment protocol. C57BL/6J mice bred under specific-pathogen-free conditions in the animal house facility at the Instituto Gulbenkian de Ciência were used to analyse the effects of streptomycin under different housing conditions. Before each experiment, male mice (aged 6–8 weeks) were first co-housed for 1 month in filter-top cages, and were then separated into cohorts of singly housed (one per cage) or co-housed (5 per cage) mice. At this stage, the mice were moved into individually ventilated cages with high-efficiency particulate air filters in our biosafety level-2 animal facility. Streptomycin (5 g l^{-1}) was maintained ad libitum in the drinking water for 15 d. Streptomycin water was replaced every 3 d. Streptomycin treatment was followed by a period of non-supplemented water, which ranged as specified according to the experiment from 4 d to 42 d before *E. coli* or *K. michiganensis* gavage. Faecal samples were collected every 5 d during streptomycin treatment, and once per week thereafter for subsequent analysis of microbiota composition. For the assessment of *E. coli* and *K. michiganensis* loads, faecal samples were obtained daily.

Ciprofloxacin treatment protocol. Conventional Swiss Webster mice (RFSW, Taconic Biosciences) were allowed to equilibrate in the Stanford mouse facility for 6 weeks. To determine the effects of ciprofloxacin treatment on the gut microbiota composition of mice housed under different conditions, 6 mice were chosen at random from a group of 11 and were singly housed thereafter; the remaining 5 mice were co-housed for the duration of the experiment. For antibiotic treatments, mice were orally gavaged for 5 d with 3 mg ciprofloxacin twice daily. Antibiotics were dissolved and administered in 200 µl of water. Mice were then followed for a further 9 d after halting ciprofloxacin treatment. Faecal samples were collected daily, at approximately the same time of day, during and after treatment for subsequent microbiota composition analysis.

Bacterial strains and strain construction. *E. coli* MG1655 derivative Sm^R, Δ*lacIZYA*::frt, Δ*lsrK*:frt strains ARO071-YFP (Δ*galK*::P_{lac}::*yfp*::*amp*), ARO073-CFP (Δ*galK*::P_{lac}::*cfp*::*amp*)[24] and VHC015-YFP Δ*gatZ* (Δ*galK*::P_{lac}::*yfp*::*amp* Δ*gatZ* Kan^R) were used. Deletion of *gatZ* from *E. coli* was introduced by bacteriophage P1-mediated transduction in ARO071[24] background as previously described[58] using lysates from strain JW2082 (ref. [59]). *K. michiganensis* ARO112 (which was isolated through plating on LB agar from a mouse faecal sample during this study), mouse commensal *E. coli* MBC064 (which was isolated through plating on LB agar from a mouse faecal sample during this study) and wild-type *S.* Typhimurium strain ATCC 14028 transformed with pMP7605-$Gent^R$-mCherry[60] (RB249) were also used in this study.

Colonization-resistance experiment. To assess the colonization-resistance capacity of co-housed versus singly housed mice, 42 d after stopping streptomycin treatment, mice were gavaged with 100 µl of PBS containing 10^8 CFUs of ARO071 (*E. coli*-YFP). Bacteria were prepared for gavage by growth to late stationary phase followed by sub-culturing to an $OD_{600} \approx 2$, corresponding to approximately 10^9 CFUs per ml. Bacteria were pelleted and resuspended in sterile PBS at this same concentration. After gavage, faecal samples were collected from each mouse daily for 9 d. Faecal material was weighed, homogenized in 1 ml of sterile PBS, diluted and plated on LB agar to determine colonization levels. Fluorescently labelled colonies were counted using a stereoscope (SteREO Lumar, Carl Zeiss) to calculate the number of *E. coli* CFUs per g faeces.

To determine the ability of *K. michiganensis* to displace or provide colonization resistance against *E. coli*, after 15 d of streptomycin treatment, singly housed mice were given either non-supplemented water for the remainder of the experiment, or non-supplemented water for 3 d and then water supplemented with 2% galactitol. Galactitol water was replaced every 2 d and prepared by dissolving galactitol powder in hot water and then allowing it to cool down before being given to mice. Then, 4 d after stopping antibiotic treatment, mice were gavaged with 100 µl of PBS containing 10^8 CFUs of either *K. michiganensis* or *E. coli*-YFP. Then, 4 d later, the mice were either not gavaged again or gavaged with 100 µl of PBS containing 10^8 CFUs of *K. michiganensis* (ARO112), *E. coli*-YFP (ARO071) or *E. coli*-CFP (ARO073). After the first gavage, faecal samples were collected from each mouse daily for 13 d. Faecal material was weighed, homogenized in 1 ml of sterile PBS, diluted and plated on LB agar supplemented with streptomycin (100 µg ml^{-1}) to determine colonization levels of *E. coli* and on LB agar to determine loads of *K. michiganensis*. The ability of *K. michiganensis* to displace *E. coli* was also tested in previously germ-free mice in which the same protocol was used with and without water supplementation with 2% galactitol. The following conditions were tested: *E. coli*-YFP colonization challenged with *K. michiganensis*;

E. coli-YFP colonization challenged with *K. michiganensis*, with galactitol added to the drinking water; *E. coli*-YFP Δ*gatZ* (VHC015) colonization challenged with *K. michiganensis*, with galactitol added to the drinking water. *E. coli*-YFP Δ*gatZ* is a strain that is impaired in galactitol consumption. Germ-free mice were bred and raised in the Gnotobiology Unit of the IGC in axenic isolators (La Calhene/ORM) and were later transferred into sterile ISOcages (Tecniplast).

To determine the ability of *K. michiganensis* or a mouse commensal *E. coli* (MBC064) to provide colonization resistance against *S.* Typhimurium, after 15 d of streptomycin treatment, singly housed mice were given non-supplemented water for the remainder of the experiment. Then, 4 d after stopping antibiotic treatment, one group of mice was gavaged with 100 µl of PBS containing 10^8 CFUs of *K. michiganensis*, another group was gavaged with 100 µl of PBS containing 10^8 CFUs of commensal *E. coli* and a final group was not gavaged. Then, 4 d after the first gavage, all of the groups were gavaged with 100 µl of PBS containing 10^4 CFUs of *S.* Typhimurium (RB249). This *S.* Typhimurium dose was chosen so that intestinal *S.* Typhimurium expansion is required, which provided time for us to follow the dynamics of colonization and infection because the mortality rate is typically high with this *S.* Typhimurium strain. After the first gavage, faecal samples were collected from each mouse daily for 13 d. Faecal material was weighed, homogenized in 1 ml of sterile PBS, diluted and plated on LB agar supplemented with gentamycin (30 µg ml^{-1}) to determine colonization levels of *S.* Typhimurium and on LB agar to determine *K. michiganensis* or commensal *E. coli* loads. According to the approved ethical protocol for animal experimentation, mice that presented extreme weight loss (20% of initial weight) or were lethargic and/or moribund due to *S.* Typhimurium infection were humanely euthanized.

***Klebsiella* detection.** A faecal sample from one mouse per cohort was collected and homogenized in 1 ml of sterile PBS. *Klebsiella* spp. are known to degrade complex plant cell wall polysaccharides, such as cellobiose, through carbohydrate-active enzymes[61]. Therefore, 5 ml of minimal medium with 0.4% cellobiose was inoculated with 100 µl of faecal suspension in glass tubes and grown overnight at 37 °C with shaking. The overnight culture was serially diluted and plated on LB agar. Ten colonies per plate with similar morphology to *Klebsiella* were streaked in Brilliance ESBL Agar (Oxoid), and 2–3 positive clones for *Klebsiella* species (according to the manufacturer's instructions) were sent for Sanger sequencing of the 16S rRNA gene, using the primers 27f (5′-GAGAGTTTGATCCTGGCTCAG-3′) and 1495r (5′-CTACGGCTACCTTGTTACGA-3′)[62] and the following reaction: 95 °C for 1 min; 30 cycles of 15 s denaturation at 95 °C, 15 s at 57 °C and 45 s at 72 °C; and extension at 72 °C for 10 min.

Whole-genome sequencing. One *Klebsiella* clone was isolated from the faeces of mouse 1 and mouse 10 (cohort 2) and grown in LB at 37 °C with agitation for subsequent DNA isolation using a previously described protocol[63]. A DNA library was constructed and sequenced at the IGC Genomics facility. Paired-end sequencing of each sample was performed using an Illumina MiSeq Benchtop Sequencer (Illumina), which produced datasets of 250 bp read pairs. *K. michiganensis* genomes have been deposited in GenBank (see Data availability). The isolates from mouse 1 and mouse 10 were greater than 97% identical to the NCBI genome sequence of *K. michiganensis* Kd70, a strain that lacks the pathogenic capacity of other *Klebsiella* spp.[43], and were 100% identical to each other.

Preparation of tissue sections for imaging. Mice were euthanized with CO_2 and death was confirmed by cervical dislocation. After euthanasia, sections of the intestinal tract (colon) were fixed using paraformaldehyde. The sections were then embedded, sectioned and stained as previously described[64]. In brief, two sections per mouse were fixed in 2% paraformaldehyde in phosphate buffer for 16–18 h, washed in 70% ethanol and then paraffin-embedded. The samples were sectioned into sections with a thickness of 4 µm for staining with DAPI, FISH probes targeting Gammaproteobacteria (Gam42A, 5′-GCCTTCCCACATCGTTT-3′) and *E. coli* (Eco1167, 5′- GCATAAGCGTCGCTGCCG-3′)[65], and lectins targeting mucin carbohydrates (Vector Laboratories). FISH was performed as previously described[64]. Gut sections collected from mice that received both *E. coli* and *K. michiganensis* were stained with 16S rRNA FISH probes that individually target Gammaproteobacteria (red) or *E. coli* specifically (green). *E. coli* cells stained with both FISH probes and therefore appeared yellow. The large, puffy diffuse green signal represented staining by the lectin Ulex Europaeus Agglutinin I (UEA1), which binds to mucus. Although the FISH probe specific for *E. coli* was also green, there were no bacteria-sized and shaped objects that appeared in only the green channel. Non-*E. coli* Gammaproteobacteria cells (red) were inferred to be *K. michiganensis* because *K. michiganensis* and *E. coli* were the dominant Gammaproteobacteria in these mice. Sections of the distal colon were imaged using a Zeiss LSM880 confocal microscope equipped with an Airyscan super-resolution module. Airyscan images were processed using Zen Blue and FIJI.

16S rRNA sequencing. For streptomycin-treatment experiments, faecal samples were stored at −80 °C and DNA extraction was performed as previously described[24]. In brief, DNA was extracted using a combination of the QIAamp Fast DNA Stool Mini Kit (Qiagen) according to the manufacturer's instructions, mechanical disruption using a tissue blender and elution to a final volume of 100 µl in ATE buffer. For each sample, the 16S rRNA gene was amplified using the 515F/806R (V4 regions) primer pairs recommended by the Earth Microbiome Project under the following PCR cycling conditions: 94 °C for 3 min; 35 cycles of 94 °C for 60 s, 50 °C for 60 s and 72 °C for 105 s; and extension at 72 °C for 10 min (refs. [66,67]). After library preparation, 2 × 250 bp sequencing was performed at the IGC Genomics Unit using an Illumina MiSeq Benchtop Sequencer.

For ciprofloxacin-treatment experiments, faecal samples were frozen and stored at −80 °C before DNA extraction. DNA was extracted from whole faecal pellets using the PowerSoil-htp kit (MO BIO). DNA extracted from faecal samples was used to generate 16S rRNA amplicons using the 515F/806R primer pairs recommended by the Earth Microbiome Project. PCR products were cleaned, quantified and pooled using the UltraClean 96 PCR Cleanup kit (MO BIO) and Quant-It dsDNA High Sensitivity Assay kit (Invitrogen). The samples were pooled and sent to the Mayo Clinic's Molecular Biology Core for 2 × 300 bp MiSeq (Illumina) library preparation and sequencing.

Sequencing data analyses. Mothur v.1.32.1 was used to process sequences as previously described[68], with some modifications. Sequences were converted to FASTA format. Sequences that were shorter than 220 bp containing homopolymers of longer than 8 bp or undetermined bases with no exact match with the forward and reverse primers, and barcodes that did not complement each other or that did not align with the appropriate 16S rRNA variable region, were not included in the analysis. A quality score above 30 (range, 0 to 40, where 0 represents an ambiguous base) was used to process sequences, which were trimmed using a sliding-window technique over a 50 bp window. Sequences were trimmed from the 3′ end until the quality score criterion was met, and were merged after that. Between 20,000 and 50,000 sequences were obtained per sample. 16S rRNA gene sequences were aligned using SILVA template reference alignment[69]. ChimeraSlayer[70] was used to remove potential chimeric sequences. Sequences with distance-based similarity of greater than 97% were joined into the same OTU using the average-neighbour algorithm. All of the samples were rarefied to the same number of sequences (10,000) for diversity analyses. Samples below 10,000 reads were removed from the analysis, which included samples from streptomycin-treated cohort 4 (mouse 11, days 0 and 57; mouse 1, day 57; mouse 6, day 57) and from the ciprofloxacin-treated cohort (mouse 9, day 5). OTU-based microbial gamma-diversity was estimated by calculating the total number of unique OTUs in each cage at each time point. In streptomycin experiments, a median value of each time point for each group was used. By contrast, for the ciprofloxacin experiment, as only one experiment was performed, the dynamic of each singly housed mouse is represented, except for mouse 9 as not all time points were available. A Bayesian classifier algorithm with a 60% bootstrap cut-off was used for each sequence[71]; sequences were assigned to the genus level where possible or otherwise to the closest genus-level classification, preceded by 'unclassified'. The Clearcut algorithm[72] was used to infer a phylogenetic tree on the basis of the 16S rRNA sequence alignment, which was used to calculate unweighted and weighted UniFrac distances between each pair of samples.

To identify OTUs with differential abundances in the microbiota of mice with and without colonization resistance to *E. coli*, we utilized the LEfSe method[42]. Abundances of the resulting OTUs that had at least 50 reads in at least two mice from one group were reanalysed for statistical significance, resulting in the elimination of OTU 45, OTU 59, OTU 75 and OTU 90. Gamma-diversity was defined as the number of unique OTUs per cage, that is, a value of unique OTUs in all 5 mice co-housed, and values of unique OTUs in each mouse singly housed.

To assess the loss of important OTUs during and after antibiotic treatment in mice under different housing conditions, we identified prevalent OTUs in untreated conditions as those represented by at least 10 reads in each untreated mouse and that were present in every mouse of each group in each cohort tested (core OTUs), and then followed the dynamics of maintenance and loss of those OTUs in the same mice both during (day 15) and after (day 57) antibiotics treatment. Samples from day 57 of mouse 1 and mouse 6 (cohort 4) had been discarded during sequencing analysis; these mice were therefore not used to analyse core OTUs.

Custom MATLAB (MathWorks) scripts were used to analyse taxa distributions across microbiota time courses.

Competition of *E. coli* and *K. michiganensis* in liquid cultures. Single colonies of *E. coli*-YFP, *E. coli*-CFP and *K. michiganensis* were used to inoculate separate 3–5 ml cultures in LB medium in glass tubes, and were grown overnight at 37 °C with shaking to an $OD_{600} \approx 5–5.5$. The overnight cultures were diluted into 96-well plates such that the total culture inoculation OD_{600} was 0.05; that is, single cultures of *E. coli*-YFP, *E. coli*-CFP, *K. michiganensis* or *S.* Typhimurium-mCherry were tested with an initial OD_{600} of 0.05, whereas co-cultures of *E. coli*-YFP + *E. coli*-CFP, *E. coli*-YFP + *K. michiganensis*, *S.* Typhimurium-mCherry + *K. michiganensis* or *S.* Typhimurium-mCherry + *E. coli*-CFP were tested with an initial OD_{600} of 0.025 of each strain. Single and co-cultures were grown in either LB medium or M9 minimal medium with a single carbon source at 0.25% (w/v). The carbon sources tested were glucose, fructose, xylose, arabinose, fucose and galactitol, as specified.

For the contact-dependent inhibition/killing assay, an overnight culture of *E. coli*-YFP was diluted into 24-well plates, and an overnight culture of *E. coli*-CFP or *K. michiganensis* was diluted into upper chambers of Transwells (0.4 µm Millicell,

Millipore) such that each chamber had an inoculation OD_{600} of 0.025. Cultures were inoculated in M9 minimal medium with arabinose or fructose at 0.25% (w/v). Furthermore, an overnight culture of *E. coli*-YFP was diluted into wells of a 96-well plate in M9 minimal medium with fructose at 0.25% (w/v) with or without supplementation of 20% cell-free spent medium. Cell-free spent medium was obtained using 0.2 µm Acrodisc syringe filters (Pall) from overnight cultures of *K. michiganensis* or *E. coli*-YFP + *K. michiganensis* grown in minimal medium with fructose at 0.25% (w/v).

All of growth curves were performed in a Thermo-Shaker Grant-bio plate reader (Thermo Fisher Scientific) without shaking at 37 °C except for the galactitol experiments, which were performed at 30 °C. Each co-culture condition was tested in six replicates across two independent experiments, and each Transwell and cell-free spent medium condition was tested in triplicate. OD_{600}, YFP fluorescence (excitation 485 nm, emission filter 535 nm; Victor3 (PerkinElmer)) and mCherry fluorescence (excitation 520 nm, emission filter 580–640 nm; Glomax Explorer (Promega)) were measured at various time points during growth, with 5 s of orbital shaking before each reading.

Single-cell imaging with propidium iodide staining. Mixed cultures of *E. coli*-YFP + *E. coli*-CFP and *E. coli*-YFP + *K. michiganensis* were grown statically for 24 h in various carbon sources. The final cultures were mixed with 10 µM of propidium iodide and incubated at room temperature for 5 min. Samples were imaged on 1% agarose pads with a Nikon Ti-E inverted microscope (Nikon Instruments) using a ×100/1.4 NA oil-immersion objective and a Zyla 5.5 sCMOS camera (Andor Technology). Images were acquired using µManager v.1.4 (http://www.micro-manager.org).

Microfluidics. Microfluidic single-cell experiments were performed using ONIX B04A microfluidic chips (CellASIC). As the microfluidic chamber selects cells by their size, the slightly larger size of *K. michiganensis* cells meant that they were less likely to get into the microfluidic viewing chamber. To address this disparity, we introduced a 10:1 ratio of *K. michiganensis* and *E. coli* cells. Before loading cells into the chamber, the cells were well mixed by alternately pressurizing wells 6 and 8 for 10 cycles. Phase-contrast and epifluorescence images were acquired using a Nikon Ti-E microscope with a ×100/1.4 NA objective and an Andor Neo 5.5 sCMOS Camera. Cells were maintained at 37 °C during imaging using an active-control environmental chamber (Haison Technology).

Growth rate analyses of microcolonies in microfluidic experiments. When introduced into the microfluidic chamber, the vast majority of cells were initially not touching any other cells. During growth, each individual cell formed a microcolony and the edges of microcolonies gradually merged. We visually identified *E. coli* microcolonies that either stayed away from any *K. michiganensis* microcolonies during $t = 2–4$ h or those with at least 50% of the periphery directly touching *K. michiganensis* cells during the same period. The $t = 2–4$ h time interval was chosen because cells grew exponentially during that period and also contained enough microcolonies in each group (isolated versus *K. michiganensis*-proximal) for statistical analysis. Microcolony areas at each time point were calculated by identifying the YFP^+ regions in the image. Growth rates were obtained by linearly fitting the slope of natural logarithm of microcolony area over time.

Quantification and statistical analyses. To determine statistically significant differences in the relative abundances of taxa and OTUs between the groups of mice, nonparametric two-tailed Mann–Whitney *U*-tests were applied using GraphPad Prism v.8. Only taxa and OTUs with at least 50 counts in at least two mice were included in the analysis. To adjust for multiple hypothesis testing, we used the Benjamini–Hochberg false-discovery rate approach[73] using the fdr.R package. Results with $P < 0.05$ or $q < 0.1$ were considered to be statistically significant. To assess significant differences in kinetic curves, we calculated the AUC for each sample using GraphPad Prism v.8, after which the AUC values for each group were evaluated using Mann–Whitney *U*-tests or Kruskal–Wallis tests with Dunn's correction for multiple comparisons. Survival assays were analysed using log-rank (Mantel–Cox) tests. To compare UniFrac distances between time points during and after treatment with streptomycin or ciprofloxacin, Mann–Whitney *U*-tests were used. Graphical representations were obtained using GraphPad Prism v.8 for Mac (https://www.graphpad.com/scientific-software/prism), MATLAB 2015b (https://www.mathworks.com/products/matlab.html) and RStudio v.3.3.3 (https://rstudio.com/products/rstudio/). Illumina sequences were analysed using Mothur v.1.32.1 (https://www.mothur.org/), which includes ChimeraSlayer and the Clearcut algorithm. The SILVA database (https://www.arb-silva.de/) was used for OTU taxonomy assignment. LEfSE OTU analysis was performed using the open-source software Galaxy (https://huttenhower.sph.harvard.edu/galaxy).

Reporting Summary. Further information on research design is available in the Nature Research Reporting Summary linked to this article.

Data availability

The *K. michiganensis* (ARO112) Whole Genome Shotgun project has been deposited at DDBJ/ENA/GenBank under the accession number WMDR00000000. The version described in this paper is version WMDR01000000. The 16S rRNA gene sequencing data (Illumina sequences) obtained in this study are available at the Sequence Read Archive (SRA) NCBI database under BioProject ID PRJNA590204. Source data are available for Figs. 1–6 and Extended Data Figs. 1–7.

Code availability

The code used for Illumina sequencing analyses in this study is available at https://github.com/mothur/mothur, with modifications that are freely available from the corresponding author on request. MATLAB routines used for data visualization are available from the corresponding author on request.

Received: 18 September 2019; Accepted: 10 December 2019;
Published online: 20 January 2020

References

1. Flint, H. J., Scott, K. P., Louis, P. & Duncan, S. H. The role of the gut microbiota in nutrition and health. *Nat. Rev. Gastroenterol. Hepatol.* **9**, 577–589 (2012).
2. Hooper, L. V., Littman, D. R. & Macpherson, A. J. Interactions between the microbiota and the immune system. *Science* **336**, 1268–1273 (2012).
3. Rakoff-Nahoum, S., Paglino, J., Eslami-Varzaneh, F., Edberg, S. & Medzhitov, R. Recognition of commensal microflora by toll-like receptors is required for intestinal homeostasis. *Cell* **118**, 229–241 (2004).
4. Ubeda, C., Djukovic, A. & Isaac, S. Roles of the intestinal microbiota in pathogen protection. *Clin. Transl. Immunol.* **6**, e128 (2017).
5. Baumler, A. J. & Sperandio, V. Interactions between the microbiota and pathogenic bacteria in the gut. *Nature* **535**, 85–93 (2016).
6. Pamer, E. G. Resurrecting the intestinal microbiota to combat antibiotic-resistant pathogens. *Science* **352**, 535–538 (2016).
7. Caporaso, J. G. et al. Moving pictures of the human microbiome. *Genome Biol.* **12**, R50 (2011).
8. Cho, I. et al. Antibiotics in early life alter the murine colonic microbiome and adiposity. *Nature* **488**, 621–626 (2012).
9. Fragiadakis, G. K. et al. Links between environment, diet, and the hunter-gatherer microbiome. *Gut Microbes* **10**, 216–227 (2018).
10. Goodrich, J. K. et al. Human genetics shape the gut microbiome. *Cell* **159**, 789–799 (2014).
11. Blaser, M. J. *Missing Microbes: How the Overuse of Antibiotics Is Fueling Our Modern Plagues* (Henry Holt and Company, 2014).
12. Sekirov, I. et al. Antibiotic-induced perturbations of the intestinal microbiota alter host susceptibility to enteric infection. *Infect. Immun.* **76**, 4726–4736 (2008).
13. Buffie, C. G. et al. Profound alterations of intestinal microbiota following a single dose of clindamycin results in sustained susceptibility to *Clostridium difficile*-induced colitis. *Infect. Immun.* **80**, 62–73 (2012).
14. Ubeda, C. et al. Vancomycin-resistant *Enterococcus* domination of intestinal microbiota is enabled by antibiotic treatment in mice and precedes bloodstream invasion in humans. *J. Clin. Invest.* **120**, 4332–4341 (2010).
15. Stecher, B. et al. *Salmonella enterica* serovar Typhimurium exploits inflammation to compete with the intestinal microbiota. *PLoS Biol.* **5**, 2177–2189 (2007).
16. Keith, J. W. & Pamer, E. G. Enlisting commensal microbes to resist antibiotic-resistant pathogens. *J. Exp. Med.* **216**, 10–19 (2019).
17. Pereira, F. C. & Berry, D. Microbial nutrient niches in the gut. *Environ. Microbiol.* **19**, 1366–1378 (2017).
18. Apperloo-Renkema, H. Z., Van der Waaij, B. D. & Van der Waaij, D. Determination of colonization resistance of the digestive tract by biotyping of Enterobacteriaceae. *Epidemiol. Infect.* **105**, 355–361 (1990).
19. Spees, A. M. et al. Streptomycin-induced inflammation enhances *Escherichia coli* gut colonization through nitrate respiration. *mBio* **4**, e00430-13 (2013).
20. Winter, S. E. et al. Host-derived nitrate boosts growth of *E. coli* in the inflamed gut. *Science* **339**, 708–711 (2013).
21. Jacobson, A. et al. A gut commensal-produced metabolite mediates colonization resistance to *Salmonella* infection. *Cell Host Microbe* **24**, 296–307 (2018).
22. Buffie, C. G. et al. Precision microbiome reconstitution restores bile acid mediated resistance to *Clostridium difficile*. *Nature* **517**, 205–208 (2014).
23. Hsiao, A. et al. Members of the human gut microbiota involved in recovery from *Vibrio cholerae* infection. *Nature* **515**, 423–426 (2014).
24. Thompson, J. A., Oliveira, R. A., Djukovic, A., Ubeda, C. & Xavier, K. B. Manipulation of the quorum sensing signal AI-2 affects the antibiotic-treated gut microbiota. *Cell Rep.* **10**, 1861–1871 (2015).
25. Cherrington, C. A., Hinton, M. & Chopra, I. Effect of short-chain organic acids on macromolecular synthesis in *Escherichia coli*. *J. Appl. Bacteriol.* **68**, 69–74 (1990).
26. Fay, J. P. & Farias, R. N. The inhibitory action of fatty acids on the growth of *Escherichia coli*. *J. Gen. Microbiol.* **91**, 233–240 (1975).
27. Kirkpatrick, C. et al. Acetate and formate stress: opposite responses in the proteome of *Escherichia coli*. *J. Bacteriol.* **183**, 6466–6477 (2001).

28. Wilson, K. H. Efficiency of various bile salt preparations for stimulation of *Clostridium difficile* spore germination. *J. Clin. Microbiol.* **18**, 1017–1019 (1983).
29. Sassone-Corsi, M. et al. Microcins mediate competition among Enterobacteriaceae in the inflamed gut. *Nature* **540**, 280–283 (2016).
30. Sana, T. G. et al. *Salmonella* Typhimurium utilizes a T6SS-mediated antibacterial weapon to establish in the host gut. *Proc. Natl Acad. Sci. USA* **113**, E5044–E5051 (2016).
31. Wexler, A. G. et al. Human symbionts inject and neutralize antibacterial toxins to persist in the gut. *Proc. Natl Acad. Sci. USA* **113**, 3639–3644 (2016).
32. Taur, Y. et al. Reconstitution of the gut microbiota of antibiotic-treated patients by autologous fecal microbiota transplant. *Sci. Transl. Med.* **10**, eaap9489 (2018).
33. Schulfer, A. F. et al. The impact of early-life sub-therapeutic antibiotic treatment (STAT) on excessive weight is robust despite transfer of intestinal microbes. *ISME J.* **13**, 1280–1292 (2019).
34. Song, S. J. et al. Cohabiting family members share microbiota with one another and with their dogs. *eLife* **2**, e00458 (2013).
35. Reese, A. T. et al. Antibiotic-induced changes in the microbiota disrupt redox dynamics in the gut. *eLife* **7**, e35987 (2018).
36. Tropini, C. et al. Transient osmotic perturbation causes long-term alteration to the gut microbiota. *Cell* **173**, 1742–1754 (2018).
37. Ng, K. M. et al. Recovery of the gut microbiota after antibiotics depends on host diet, community context, and environmental reservoirs. *Cell Host Microbe* **26**, 650–665 (2019).
38. Velazquez, E. M. et al. Endogenous Enterobacteriaceae underlie variation in susceptibility to *Salmonella* infection. *Nat. Microbiol.* **4**, 1057–1064 (2019).
39. Franklin, C. L. & Ericsson, A. C. Microbiota and reproducibility of rodent models. *Lab Anim.* **46**, 114–122 (2017).
40. Barthel, M. et al. Pretreatment of mice with streptomycin provides a *Salmonella enterica* serovar Typhimurium colitis model that allows analysis of both pathogen and host. *Infect. Immun.* **71**, 2839–2858 (2003).
41. Leatham, M. P. et al. Precolonized human commensal *Escherichia coli* strains serve as a barrier to *E. coli* O157:H7 growth in the streptomycin-treated mouse intestine. *Infect. Immun.* **77**, 2876–2886 (2009).
42. Segata, N. et al. Metagenomic biomarker discovery and explanation. *Genome Biol.* **12**, R60 (2011).
43. Dantur, K. I. et al. The endophytic strain *Klebsiella michiganensis* Kd70 lacks pathogenic island-like regions in its genome and is incapable of infecting the urinary tract in mice. *Front. Microbiol.* **9**, 1548 (2018).
44. Conway, T. & Cohen, P. S. Commensal and pathogenic *Escherichia coli* metabolism in the Gut. *Microbiol. Spectr.* **3**, MBP-0006-2014 (2015).
45. Flint, H. J., Scott, K. P., Duncan, S. H., Louis, P. & Forano, E. Microbial degradation of complex carbohydrates in the gut. *Gut Microbes* **3**, 289–306 (2012).
46. Saha, R., Farrance, C. E., Verghese, B., Hong, S. & Donofrio, R. S. *Klebsiella michiganensis* sp. nov., a new bacterium isolated from a tooth brush holder. *Curr. Microbiol.* **66**, 72–78 (2013).
47. Barroso-Batista, J. et al. The first steps of adaptation of *Escherichia coli* to the gut are dominated by soft sweeps. *PLoS Genet.* **10**, e1004182 (2014).
48. Maltby, R., Leatham-Jensen, M. P., Gibson, T., Cohen, P. S. & Conway, T. Nutritional basis for colonization resistance by human commensal *Escherichia coli* strains HS and Nissle 1917 against *E. coli* O157:H7 in the mouse intestine. *PLoS ONE* **8**, e53957 (2013).
49. Stecher, B. et al. Like will to like: abundances of closely related species can predict susceptibility to intestinal colonization by pathogenic and commensal bacteria. *PLoS Pathog.* **6**, e1000711 (2010).
50. Kamada, N. et al. Regulated virulence controls the ability of a pathogen to compete with the gut microbiota. *Science* **336**, 1325–1329 (2012).
51. Deriu, E. et al. Probiotic bacteria reduce *Salmonella* typhimurium intestinal colonization by competing for iron. *Cell Host Microbe* **14**, 26–37 (2013).
52. Herp, S. et al. *Mucispirillum schaedleri* antagonizes *Salmonella* virulence to protect mice against colitis. *Cell Host Microbe* **25**, 681–694 (2019).
53. Jernberg, C., Löfmark, S., Edlund, C. & Jansson, J. K. Long-term impacts of antibiotic exposure on the human intestinal microbiota. *Microbiology* **156**, 3216–3223 (2010).
54. Clemente, J. C. et al. The microbiome of uncontacted Amerindians. *Sci. Adv.* **1**, e1500183 (2015).
55. Martinez, I. et al. The gut microbiota of rural Papua New Guineans: composition, diversity patterns, and ecological processes. *Cell Rep.* **11**, 527–538 (2015).
56. van Nood, E. et al. Duodenal infusion of donor feces for recurrent *Clostridium difficile*. *N. Engl. J. Med.* **368**, 407–415 (2013).
57. Dominguez-Bello, M. G. et al. Partial restoration of the microbiota of cesarean-born infants via vaginal microbial transfer. *Nat. Med.* **22**, 250–253 (2016).
58. Silhavy, T. J., Berman, M. L. & Enquist, L. W. (eds) *Experiments with Gene Fusions* (Cold Spring Harbor Laboratory, 1984).
59. Baba, T. et al. Construction of *Escherichia coli* K-12 in-frame, single-gene knockout mutants: the Keio collection. *Mol. Syst. Biol.* **2**, 2006.0008 (2006).
60. Shyntum, D. Y. et al. *Pantoea ananatis* utilizes a type VI secretion system for pathogenesis and bacterial competition. *Mol. Plant Microbe Interact.* **28**, 420–431 (2015).
61. Yu, Z. et al. Complete genome sequence of N_2-fixing model strain *Klebsiella* sp. nov. M5al, which produces plant cell wall-degrading enzymes and siderophores. *Biotechnol. Rep.* **17**, 6–9 (2018).
62. Bianciotto, V. et al. An obligately endosymbiotic mycorrhizal fungus itself harbors obligately intracellular bacteria. *Appl. Environ. Microbiol.* **62**, 3005–3010 (1996).
63. Wilson, K. Preparation of genomic DNA from bacteria. *Curr. Protoc. Mol. Biol.* **56**, 2.4.1–2.4.5 (2001).
64. Earle, K. A. et al. Quantitative imaging of gut microbiota spatial organization. *Cell Host Microbe* **18**, 478–488 (2015).
65. Dejea, C. M. et al. Microbiota organization is a distinct feature of proximal colorectal cancers. *Proc. Natl Acad. Sci. USA* **111**, 18321–18326 (2014).
66. Caporaso, J. G. et al. Ultra-high-throughput microbial community analysis on the Illumina HiSeq and MiSeq platforms. *ISME J.* **6**, 1621–1624 (2012).
67. Caporaso, J. G. et al. Global patterns of 16S rRNA diversity at a depth of millions of sequences per sample. *Proc. Natl Acad. Sci. USA* **108**(Suppl), 4516–4522 (2011).
68. Kozich, J. J., Westcott, S. L., Baxter, N. T., Highlander, S. K. & Schloss, P. D. Development of a dual-index sequencing strategy and curation pipeline for analyzing amplicon sequence data on the MiSeq Illumina sequencing platform. *Appl. Environ. Microbiol.* **79**, 5112–5120 (2013).
69. Pruesse, E. et al. SILVA: a comprehensive online resource for quality checked and aligned ribosomal RNA sequence data compatible with ARB. *Nucleic Acids Res.* **35**, 7188–7196 (2007).
70. Haas, B. J. et al. Chimeric 16S rRNA sequence formation and detection in Sanger and 454-pyrosequenced PCR amplicons. *Genome Res.* **21**, 494–504 (2011).
71. Wang, Q., Garrity, G. M., Tiedje, J. M. & Cole, J. R. Naive Bayesian classifier for rapid assignment of rRNA sequences into the new bacterial taxonomy. *Appl. Environ. Microbiol.* **73**, 5261–5267 (2007).
72. Sheneman, L., Evans, J. & Foster, J. A. Clearcut: a fast implementation of relaxed neighbor joining. *Bioinformatics* **22**, 2823–2824 (2006).
73. Benjamini, Y. & Hochberg, Y. Controlling the false discovery rate: a practical and powerful approach to multiple testing. *Proc. R. Soc. B* **57**, 289–300 (1995).

Acknowledgements

We thank T. Sana, E. Cascales and M. Blokesch for helpful discussions; J. Xavier, C. Ubeda and M. Taga for suggestions and for reading the manuscript; S. Higginbottom for help with mouse experiments; and R. Balbontín-Soria for providing strain RB249. We acknowledge support from the Allen Discovery Center at Stanford on Systems Modeling of Infection (to K.M.N. and K.C.H.); the Portuguese national funding agency Fundação para a Ciência e Tecnologia (FCT) PTDC/BIA-MIC/4188/14 and research infrastructure ONEIDA and CONGENTO projects (LISBOA-01-0145-FEDER-016417 and LISBOA-01-0145-FEDER-022170) co-funded by Fundos Europeus Estruturais e de Investimento from Programa Operacional Regional Lisboa 2020 (to R.A.O. and K.B.X.). K.B.X., R.A.O. and V.C. acknowledge the FCT for individual grants IF/00831/2015, PD/BD/106000/2014 and SFRH/BPD/116806/2016, respectively. J.L.S. and K.C.H. are Chan Zuckerberg Biohub Investigators.

Author contributions

R.A.O. performed and analysed streptomycin treatment and gnotobiotic mice experiments with assistance from V.C. and supervision from K.B.X. K.M.N. performed ciprofloxacin-treatment mouse experiments, with supervision by K.C.H. and J.L.S. R.A.O. and K.M.N. performed microbiota analyses. R.A.O., M.B.C. and V.C. performed bacterial growth curves. H.S. performed and analysed microfluidics experiments and single-cell imaging. R.A.O. and V.C. prepared tissue sections and K.M.N. performed imaging analyses. R.A.O., K.C.H. and K.B.X. designed the study and wrote the original draft of the paper. All of the other authors contributed to writing the manuscript.

Competing interests

The authors declare no competing interests.

Additional information

Extended data is available for this paper at https://doi.org/10.1038/s41564-019-0658-4.

Supplementary information is available for this paper at https://doi.org/10.1038/s41564-019-0658-4.

Correspondence and requests for materials should be addressed to K.B.X.

Reprints and permissions information is available at www.nature.com/reprints.

Publisher's note Springer Nature remains neutral with regard to jurisdictional claims in published maps and institutional affiliations.

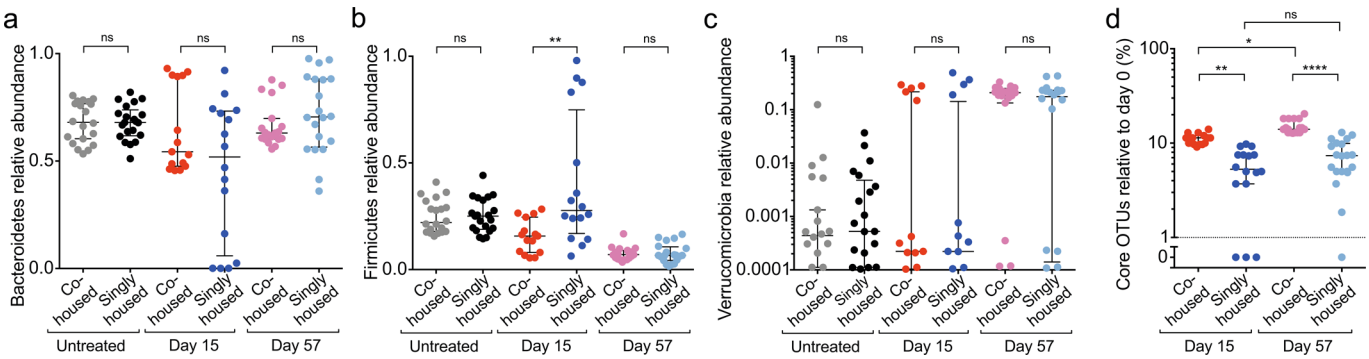

Extended Data Fig. 1 | Streptomycin treatment leads to increased loss of core OTUs in singly housed mice compared to co-housed mice, but does not differentially affect Bacteroidetes, Firmicutes, or Verrucomicrobia relative abundances. a–**c**, Relative abundances of the a, Bacteroidetes, **b**, Firmicutes and c, Verrucomicrobia phyla in co-housed and singly housed mice at indicated time points. Data shown are medians, and error bars show the interquartile range of *n*=15-21 per group. **d**, Percentage of core OTUs (defined as OTUs present in every mouse of each group before treatment) present on days 15 and 57, relative to day 0. Data from **a**–**c** represent *n*=20 co-housed mice and *n*=21 singly housed mice from 4 independent experiments. Data in d represent *n*=3 cages (day 15) or *n*=4 cages (day 57) of co-housed mice and *n*=21 (day 15) or *n*= 15 (day 57) singly housed mice from 3 (day 15) or 4 (day 57) independent experiments. Lines in **a**–**d** represent medians and error bars depict interquartile ranges. Data in a-c were analyzed with two-tailed Mann-Whitney test (**: $p<0.01$; ns, not significant). For **d**, data were analyzed using the one-way Kruskal-Wallis test with Dunn's correction test for multiple comparisons (*: $q < 0.1$, **: $q < 0.05$; ****: $q < 0.001$; ns, not significant).

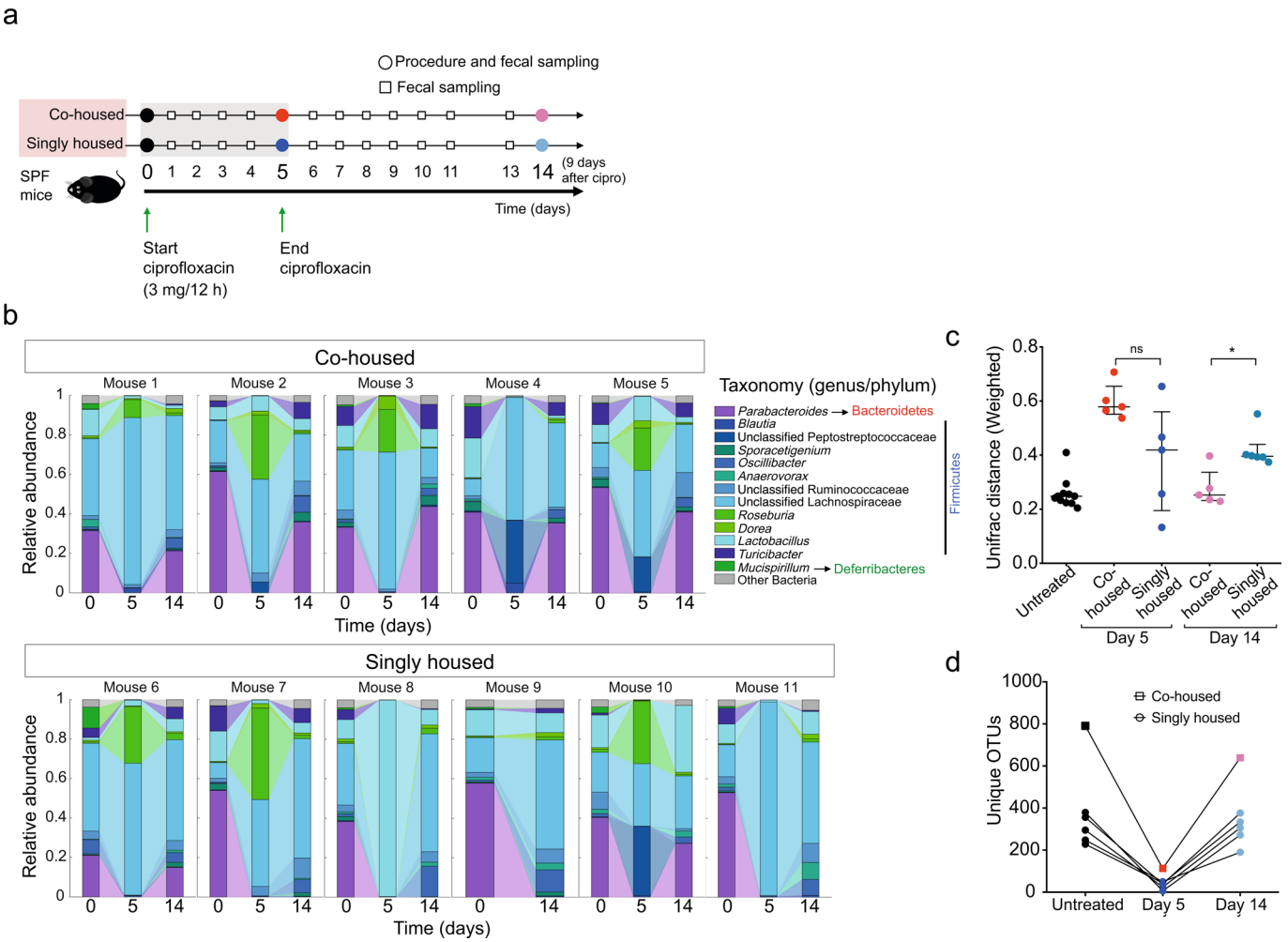

Extended Data Fig. 2 | Ciprofloxacin treatment results in stochastic extinction of the Bacteroidetes phylum in singly housed mice. a, Experimental scheme for ciprofloxacin treatment, from one experiment. Three milligrams of ciprofloxacin were administered orally every 12 h to conventional Swiss Webster mice for 5 days. Microbiota composition was analyzed from fecal samples collected from day 0 (before antibiotics), day 5 (last day of antibiotic treatment), and day 14 (9 days after stopping antibiotic treatment). Procedures (circles) denote the start (day 0) or the end (day 5) of ciprofloxacin treatment, and sacrifice mice (day 14). **b**, Fecal microbiota compositions on day 0, 5, and 14 of co-housed (Mouse 1-5) and singly housed (Mouse 6-11) mice. Each stacked bar represents the microbiota composition in the indicated mouse at the indicated time points. The colored segments represent the relative fraction of each genus-level taxon present at >3%. All other genera were combined in the "Other Bacteria" category. **c**, Phylogenetic dissimilarities on each day determined by the mean weighted Unifrac distance of the bacterial communities of each mouse to each other mouse within the same group. Data shown are medians, and the error bars show interquartile ranges (*: $p<0.05$; ns: not significant; two-tailed Mann-Whitney test, $n=5$ mice in the co-housed group, $n=6$ mice in the singly housed group). **d**, Gamma diversity of gut microbiota of co-housed and singly housed mice at indicated time points ($n=1$ cage in co-housed group, $n=5$ mice in singly housed group).

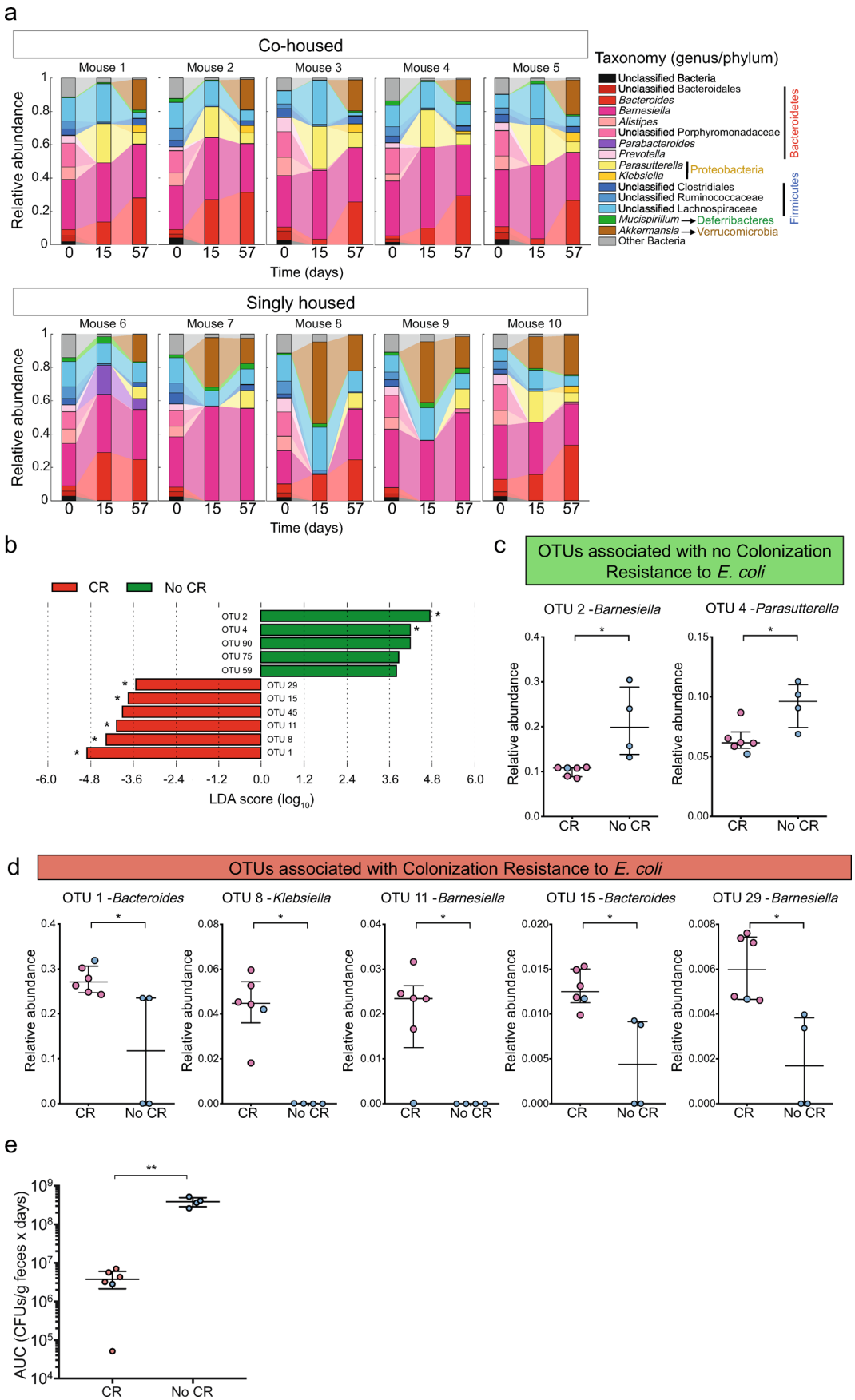

Extended Data Fig. 3 | See next page for caption.

Extended Data Fig. 3 | Effects of streptomycin treatment on microbiota composition and OTUs associated with colonization resistance to *E. coli* in cohort 2 (associated with the experiments shown in Figs. 1 and 2). a, Fecal microbiota compositions of untreated (day 0), streptomycin-treated (day 15), and post-streptomycin-treated (day 57) samples from co-housed and singly housed mice in cohort 2. Each stacked bar represents the microbiota composition in one mouse at the indicated time points. Colored segments represent the relative fraction of each genus-level bacterial taxon present at >3%. All other genera were combined into the "Other Bacteria" category. **b**, Histogram of linear discriminant analysis (LDA) scores >2 for differentially abundant OTUs on day 57 of mice in cohort 2 from the experiment in Fig. 2c, d. Red designates OTUs enriched in mice with colonization resistance to *E. coli* (CR); green designates OTUs enriched in mice lacking colonization resistance (No CR). **c**, Relative abundances of significantly different individual OTUs that are associated with lack of colonization resistance against *E. coli*. **d**, Relative abundances of significantly different individual OTUs that are associated with colonization resistance against *E. coli*. e, Area Under the Curve (AUC) calculated from the dynamics of *E. coli*-YFP CFUs/*g* feces during the cohort 2 experiment of each mouse with and without colonization resistance shows that *Klebsiella*-associated mice had significantly lower loads of *E. coli* throughout the experiment. Data in **b**–**e** represent n=6 CR mice and n=4 No CR mice from 1 experiment. In **c**–**e**, medians and interquartile ranges are shown. In **b**, LEfSe uses the Kruskal-Wallis rank-sum test on a normalized relative abundance matrix to detect significantly different OTU features and estimates the effect size of each feature via LDA; only features with LDA scores >2 and alpha<0.05 were considered different between the groups of mice and are shown. Asterisks (*) in b represent statistical results from c and d. Data in **c** and **d** were analyzed with two-tailed Wilcoxon test using a Benjamini-Hochberg correction for multiple comparisons (∗: q<0.1). Data in e were analyzed with two-tailed Mann-Whitney test (**: p<0.01).

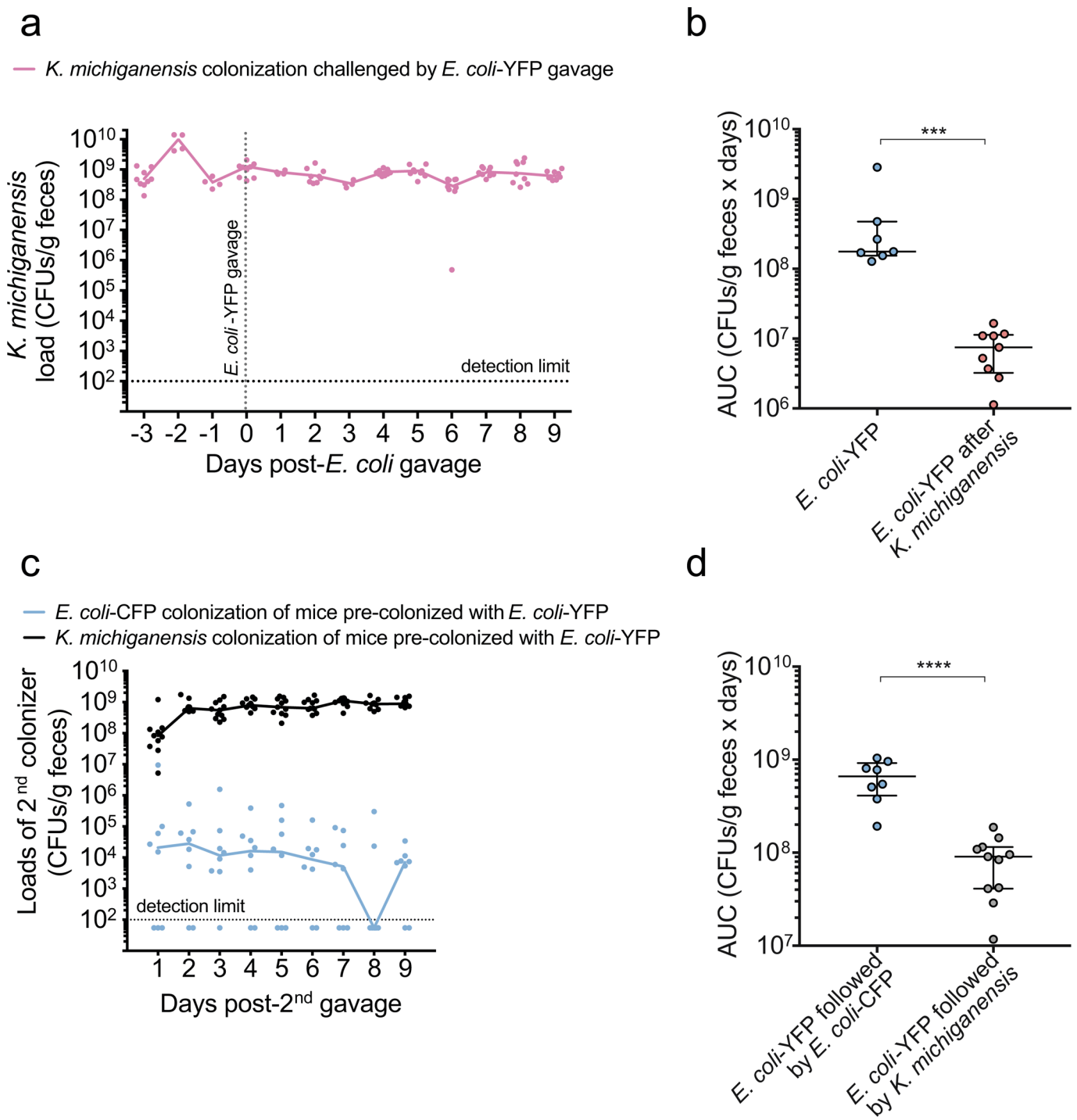

Extended Data Fig. 4 | *K. michiganensis* and *E. coli*-CFP colonization loads from experiment in Fig. 3c–e. a, Loads of *K. michiganensis* (CFUs/g feces) before and after challenge with *E. coli*-YFP (n=9 across two independent experiments, Fig. 3d). **b**, Area Under the Curve (AUC) calculated from the dynamics of *E. coli*-YFP CFUs/g feces of each mouse with and without *K. michiganensis*. Mice associated with *K. michiganensis* had significantly lower loads of *E. coli* throughout the experiment (n=9 across two independent experiments, Fig. 3d). **c**, *K. michiganensis* (n=11 across three independent experiments) and *E. coli*-CFP (n=8 across two independent experiments) loads (CFUs/g feces) in mice pre-colonized with *E. coli*-YFP (Fig. 3c, e). **d**, AUC calculated from the dynamics of *E. coli*-YFP CFUs/g feces of each mouse after challenge with *K. michiganensis* or *E. coli*-CFP. Mice challenged with *K. michiganensis* had significantly lower loads of *E. coli* throughout the experiment (n=11 across three independent experiments) as compared to challenge with *E. coli*-CFP (n=8 across two independent experiments; Fig. 3e). In a and **c**, circles and lines represent values from individual mice and medians, respectively. In **b** and **d**, medians and interquartile ranges are shown. Data in **b** and **d** were analyzed with the two-tailed Mann-Whitney test (***: p<0.001; ****: p<0.0001).

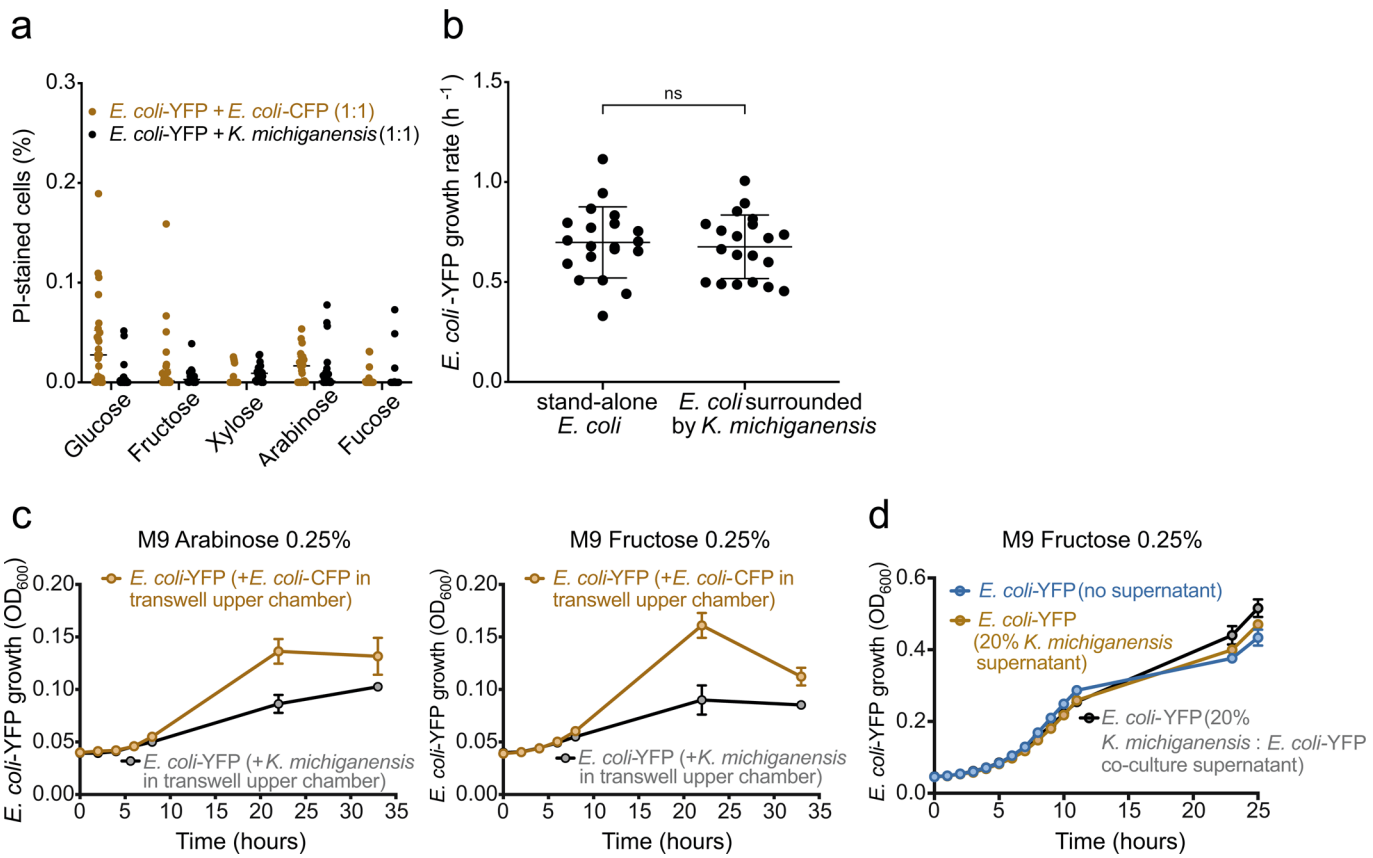

Extended Data Fig. 5 | No killing of *E. coli* or direct physical inhibition by *K. michiganensis* was observed *in vitro*. **a**, Co-cultures of *E. coli*-YFP with *E. coli*-CFP or *K. michiganensis* in minimal media containing 0.25% of the indicated carbon source exhibited similar percentages of PI-stained cells, suggesting the absence of active killing of *E. coli*. **b**, There was no statistically significant difference in the growth rates of *E. coli* microcolonies that were well separated from versus surrounded by *K. michiganensis* cells over >50% of the periphery in minimal medium with arabinose. **c**, Cell density of *E. coli*-YFP in the bottom chamber of a transwell incubated with *K. michiganensis* or *E. coli*-CFP in the upper chamber in minimal media with arabinose or fructose. Growth was monitored by OD_{600} measurements for 35 h (n=3 per condition). **d**, Cell density of *E. coli*-YFP in minimal medium with fructose with or without supplementation of 20% cell-free spent medium from overnight cultures of *K. michiganensis* or *E. coli*-YFP+*K. michiganensis* grown in minimal medium with fructose. Growth was monitored by OD_{600} measurements for 25 h (n=3 per condition). Data in **b** were analyzed with two-tailed Mann-Whitney test (ns: not significant). Lines and error bars in **b**-**d** represent means and standard deviations, respectively.

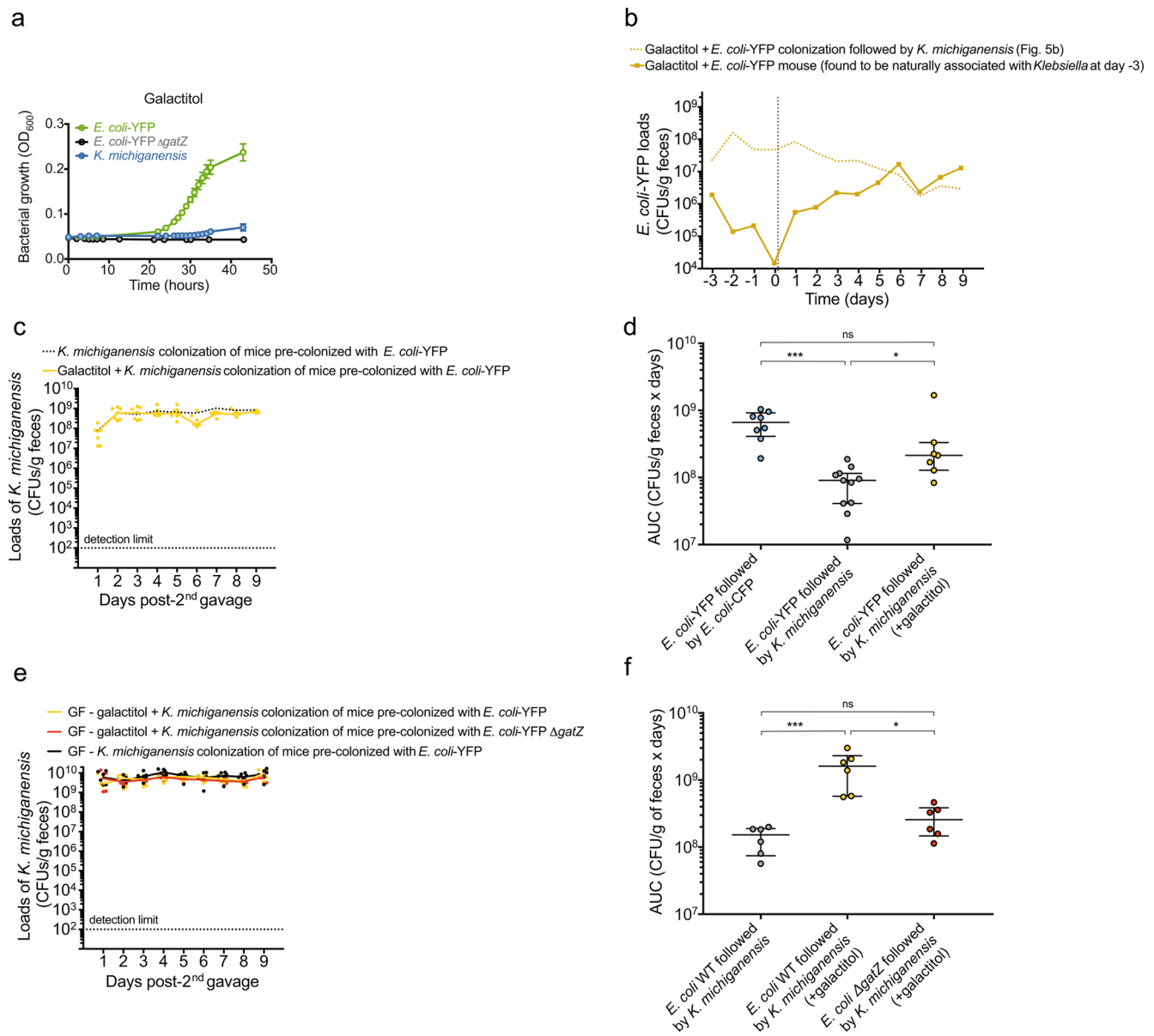

Extended Data Fig. 6 | Galactitol can sustain growth of *E. coli*-YFP but not *K. michiganensis in vitro*; *E. coli*-YFP colonization of a singly housed mouse in which *Klebsiella* spp. were not eliminated by streptomycin treatment, and loads of the 2nd colonizer from the experiment shown in Fig. 5. a, Growth capacity of *K. michiganensis*, *E. coli*-YFP, and *E. coli*-YFP Δ*gatZ* alone in minimal medium containing 0.25% galactitol. Growth was monitored by OD_{600} measurements at the indicated times for 43 h (n=6 per condition). *K. michiganensis* and *E. coli*-YFP Δ*gatZ* were unable to grow on galactitol, by contrast to *E. coli*-YFP. **b**, While measuring the capacity of galactitol to affect *K. michiganensis*-mediated colonization resistance against *E. coli* in singly housed mice after streptomycin treatment, we noted that one mouse presented high levels of resident *Klebsiella* spp. In this mouse, *E. coli*-YFP loads (CFUs/g feces) decreased immediately after gavage (day -3) (yellow solid line). This mouse was not included in the data displayed in Fig. 5b (see Supplementary Discussion). These data are from n=1 mouse from one experiment. Dashed yellow line shows the median CFUs/g feces of *E. coli*-YFP from Fig. 5b for comparison. **c**, Yellow line shows *K. michiganensis* loads (CFUs/g feces) in mice pre-colonized with *E. coli*-YFP and drinking water supplemented with 2% galactitol (n=7 across two independent experiments, Fig. 5a). Black dashed line shows median CFUs/g feces of *K. michiganensis* from the experiment in Fig. 2c, e for comparison (Extended Data Fig. 4c). **d**, Area Under the Curve (AUC) calculated from the dynamics of *E. coli*-YFP CFUs/g feces of each mouse drinking galactitol-supplemented water after challenge with *K. michiganensis* (n=7 across two independent experiments, Fig. 5b) compared with dynamics of *E. coli*-YFP CFUs/g feces of each mouse drinking non-supplemented water with and without *K. michiganensis* (data from Extended Data Fig. 4d) . Mice drinking galactitol-supplemented water had significantly higher *E. coli* loads throughout the experiment when compared with mice drinking non-supplemented water, even in the presence of *K. michiganensis*. **e**, *K. michiganensis* loads (CFUs/g feces) in ex-germ-free mice pre-colonized with *E. coli*-YFP or *E. coli*-YFP Δ*gatZ* drinking non-supplemented or 2% galactitol-supplemented water (n=6 per condition across two independent experiments, Fig. 5c). **f**, AUC calculated from the dynamics of *E. coli*-YFP CFUs/g feces of each ex-germ-free mouse drinking non-supplemented or 2% galactitol-supplemented water after challenge with *K. michiganensis* (n=6 per group across two independent experiments, Fig. 5d). Mice drinking galactitol-supplemented water had significantly higher *E. coli*-YFP loads throughout the experiment when compared with mice drinking non-supplemented water or *E. coli*-YFP Δ*gatZ* in mice drinking galactitol-supplemented water, even in the presence of *K. michiganensis*. Data in a represent means and standard deviations. In **c** and **e**, circles and lines represent values from individual mice and medians, respectively. In d and f, medians and interquartile ranges are shown. In d and f, data were analyzed using the Kruskal-Wallis test with Dunn's correction test for multiple comparison (*: q<0.1; ***: q<0.01; ns, not significant).

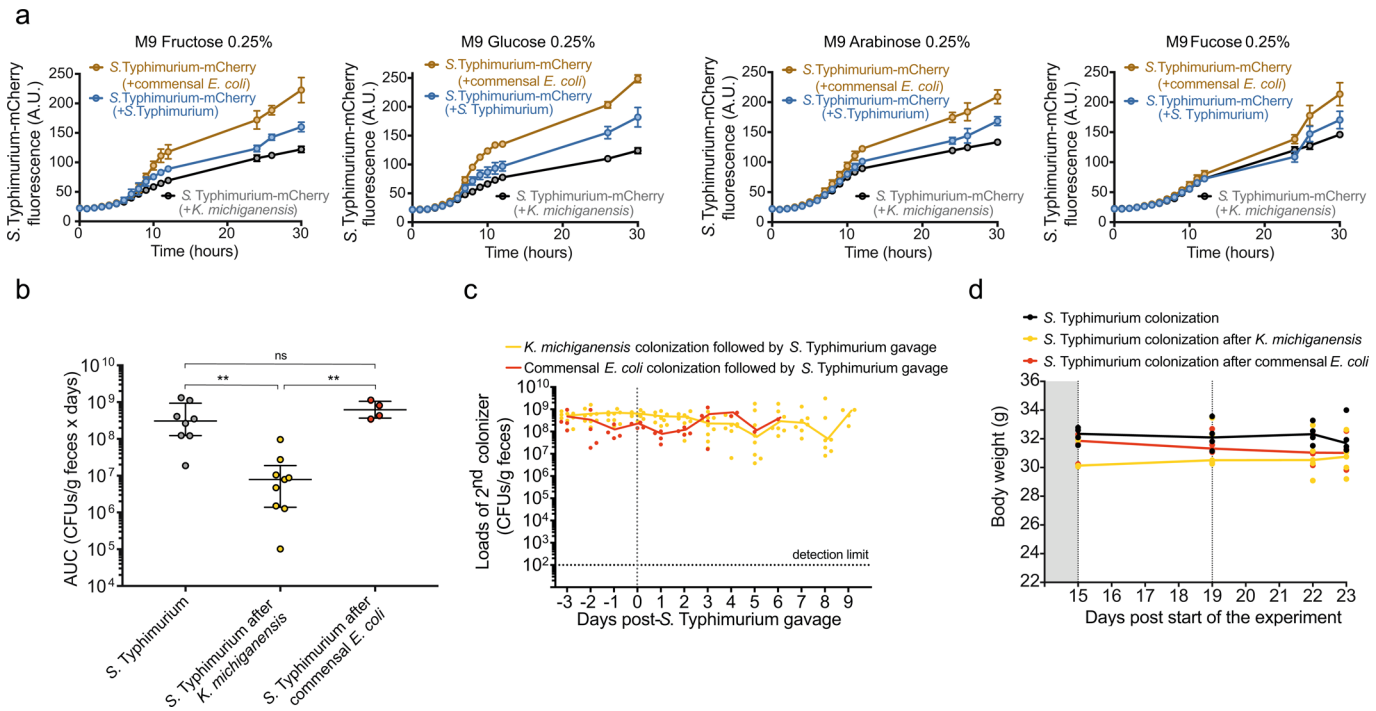

Extended Data Fig. 7 | Competition for simple sugars by *K. michiganensis* and commensal *E. coli* with *S.* Typhimurium, and colonization loads of *K. michiganensis* and commensal *E. coli* from the experiment in Fig. 6. a, *S.* Typhimurium-mCherry growth capacity in co-cultures with *K. michiganensis*, commensal *E. coli* or an isogenic *S.* Typhimurium (without a fluorescent-protein marker) in minimal media containing 0.25% of the indicated carbon source. *S.* Typhimurium-mCherry growth was monitored by mCherry fluorescence quantification (n=6 per condition). **b**, Area Under the Curve (AUC) calculated from the dynamics of *S.* Typhimurium CFUs/g feces of each mouse in the first 3 days after *S.* Typhimurium challenge in mice pre-colonized with *K. michiganensis* (n=9 across 2 independent experiments), as compared to mice not pre-colonized or pre-colonized with a commensal *E. coli* (n=8 across 2 independent experiments and n=4 in 1 experiment, respectively; Fig. 6). Mice colonized with *K. michiganensis* had significantly lower *S.* Typhimurium loads as compared to mice not pre-colonized or pre-colonized with a commensal *E. coli*. **c**, Loads of *K. michiganensis* (n=9 mice across two independent experiments) and commensal *E. coli* (n=4 mice, from one experiment) in CFUs/g feces before and after challenge with *S.* Typhimurium (Fig. 6b). **d**, Mice body weight from day 19 to 23 was unaffected by *K. michiganensis* (n=5 mice from one experiment), commensal *E. coli* (n=4 mice from one experiment) colonization, similarly to non-challenged. In **a**, lines and error bars represent means and standard deviations, respectively. In **b**, lines and errors bars represent medians and interquartile ranges, respectively. Data in **b** were analyzed using the one-sided Kruskal-Wallis test with Dunn's correction test for multiple comparisons (**: $q < 0.05$; ns, not significant). In **c** and **d**, circles and lines represent values from individual mice and medians, respectively.

nature research

Corresponding author(s): Karina B. Xavier

Last updated by author(s): Nov 21, 2019

Reporting Summary

Nature Research wishes to improve the reproducibility of the work that we publish. This form provides structure for consistency and transparency in reporting. For further information on Nature Research policies, see Authors & Referees and the Editorial Policy Checklist.

Statistics

For all statistical analyses, confirm that the following items are present in the figure legend, table legend, main text, or Methods section.

n/a	Confirmed
☐	☒ The exact sample size (*n*) for each experimental group/condition, given as a discrete number and unit of measurement
☐	☒ A statement on whether measurements were taken from distinct samples or whether the same sample was measured repeatedly
☐	☒ The statistical test(s) used AND whether they are one- or two-sided *Only common tests should be described solely by name; describe more complex techniques in the Methods section.*
☒	☐ A description of all covariates tested
☐	☒ A description of any assumptions or corrections, such as tests of normality and adjustment for multiple comparisons
☐	☒ A full description of the statistical parameters including central tendency (e.g. means) or other basic estimates (e.g. regression coefficient) AND variation (e.g. standard deviation) or associated estimates of uncertainty (e.g. confidence intervals)
☐	☒ For null hypothesis testing, the test statistic (e.g. *F*, *t*, *r*) with confidence intervals, effect sizes, degrees of freedom and *P* value noted *Give P values as exact values whenever suitable.*
☒	☐ For Bayesian analysis, information on the choice of priors and Markov chain Monte Carlo settings
☒	☐ For hierarchical and complex designs, identification of the appropriate level for tests and full reporting of outcomes
☒	☐ Estimates of effect sizes (e.g. Cohen's *d*, Pearson's *r*), indicating how they were calculated

Our web collection on statistics for biologists contains articles on many of the points above.

Software and code

Policy information about availability of computer code

Data collection	Perkin Elmer 2030 Workstation was used to operate the plate reader for measurement of OD600 and YFP expression in sinlge- and co-cultures. GloMax Explorer was used to operate the plate reader for measurement of OD600 and mCherry expression in sinlge- and co-cultures. Zen Blue and FIJI were used to process fluorescence microscopy images. micro-Manager was used to acquire single-cell images.
Data analysis	Graphical representations were obtained using Graphpad Prism v. 8 for Mac (https://www.graphpad.com/scientific-software/prism), MATLAB 2015b (https://www.mathworks.com/products/matlab.html), and RStudio v. 3.3.3 (https://rstudio.com/products/rstudio/). Illumina sequences were analyzed using Mothur v. 1.32.1 (https://www.mothur.org/), which includes ChimeraSlayer and Clearcut algorithms, and RStudio. SILVA database (https://www.arb-silva.de/) was used for OTU taxonomy assignment. LEfSE OTU analysis was performed using the open-source software Galaxy (https://huttenhower.sph.harvard.edu/galaxy).

For manuscripts utilizing custom algorithms or software that are central to the research but not yet described in published literature, software must be made available to editors/reviewers. We strongly encourage code deposition in a community repository (e.g. GitHub). See the Nature Research guidelines for submitting code & software for further information.

Data

Policy information about availability of data

All manuscripts must include a data availability statement. This statement should provide the following information, where applicable:

- Accession codes, unique identifiers, or web links for publicly available datasets
- A list of figures that have associated raw data
- A description of any restrictions on data availability

All analysis codes are available from the corresponding author upon request. Klebsiella michiganensis (ARO112) Whole Genome Shotgun project has been deposited at DDBJ/ENA/GenBank under the accession number WMDR00000000. The version described in this paper is version WMDR01000000. The 16S rRNA gene sequencing data (Illumina sequences) obtained in this study are available at Sequence Read Archives (SRA) NCBI database under BioProject ID number PRJNA590204.

Field-specific reporting

Please select the one below that is the best fit for your research. If you are not sure, read the appropriate sections before making your selection.

☒ Life sciences ☐ Behavioural & social sciences ☐ Ecological, evolutionary & environmental sciences

For a reference copy of the document with all sections, see nature.com/documents/nr-reporting-summary-flat.pdf

Life sciences study design

All studies must disclose on these points even when the disclosure is negative.

Sample size	From 4-21 mice were used in each group. Sample size was chosen according to institutional directives and in accordance with the 3Rs rules (Replacement, Reduction and Refinement) guiding principles underpinning the humane use of animals in research, but no statistical analyses were performed to predetermine the sample sizes. N=4 is the minimum number of independent subjects to be used for statistical analysis to be performed.
Data exclusions	No data were excluded from the analysis. One mouse was removed from the galactitol treatment group (Fig. 5a,b), due to stochastic maintenance of a native Klebsiella spp and the data from this mouse is therefore presented as such in the supplementary data (Supplementary Fig. 4).
Replication	All attempts at replication were successful, with multiple mice in each group (see sample size above).All experiments were done at least twice, with the exception of in vivo experiment with commensal E. coli and the ciprofloxacin-treatment experiment, which were done only once.
Randomization	Mice were randomly allocated to different treatments. We ensured that in each experiment all mice were siblings and shared the same cage for microbiome homogenization prior to the experiment.
Blinding	Blinding does not apply to this study because the investigators needed to identify the cages of mice for subsequent colonization resistance tests.

Reporting for specific materials, systems and methods

We require information from authors about some types of materials, experimental systems and methods used in many studies. Here, indicate whether each material, system or method listed is relevant to your study. If you are not sure if a list item applies to your research, read the appropriate section before selecting a response.

Materials & experimental systems

n/a	Involved in the study
☒	☐ Antibodies
☒	☐ Eukaryotic cell lines
☒	☐ Palaeontology
☐	☒ Animals and other organisms
☒	☐ Human research participants
☒	☐ Clinical data

Methods

n/a	Involved in the study
☒	☐ ChIP-seq
☒	☐ Flow cytometry
☒	☐ MRI-based neuroimaging

Animals and other organisms

Policy information about studies involving animals; ARRIVE guidelines recommended for reporting animal research

Laboratory animals	6- to 8-week old C57BL/6 male mice (in-house bred, original breeding pairs from Charles River Laboratories) and 10-week old Swiss-Webster male mice from Taconic Biosciences were used, as specified in the text.
Wild animals	No wild animals were used.
Field-collected samples	This study did not involve samples collected from the field.
Ethics oversight	All experiments performed with C57BL/6 mice were included in an animal experimentation protocol approved by IGC ethics committee and the Portuguese Nacional Entity (DGAV) - Protocol number 015190. All experiments performed with SW mice were performed in accordance with the Administrative Panel on Laboratory Animal Care , Standford University's IACUC.

Note that full information on the approval of the study protocol must also be provided in the manuscript.